# E4BP4-mediated inhibition of T follicular helper cell differentiation is compromised in autoimmune diseases

Zijun Wang,[1,2] Ming Zhao,[1,2] Jinghua Yin,[1,2] Limin Liu,[1,2] Longyuan Hu,[1,2] Yi Huang,[1,2] Aiyun Liu,[1,2] Jiajun Ouyang,[1,2] Xiaoli Min,[1,2] Shijia Rao,[1,2] Wenhui Zhou,[1,2] Haijing Wu,[1,2] Akihiko Yoshimura,[3] and Qianjin Lu[1,2]

[1]Department of Dermatology, Hunan Key Laboratory of Medical Epigenomics, The Second Xiangya Hospital, Central South University, Changsha, China. [2]Research Unit of Key Technologies of Diagnosis and Treatment for Immune-related Skin Diseases, Chinese Academy of Medical Sciences, Changsha, China. [3]Department of Microbiology and Immunology, Keio University School of Medicine, Tokyo, Japan.

**T follicular helper (Tfh) cells are indispensable for the formation of germinal center (GC) reactions, whereas T follicular regulatory (Tfr) cells inhibit Tfh-mediated GC responses. Aberrant activation of Tfh cells contributes substantially to the pathogenesis of autoimmune diseases, such as systemic lupus erythematosus (SLE). Nonetheless, the molecular mechanisms mitigating excessive Tfh cell differentiation are not fully understood. Herein we demonstrate that the adenovirus E4 promoter-binding protein (E4BP4) mediates a feedback loop and acts as a transcriptional brake to inhibit Tfh cell differentiation. Furthermore, we show that such an immunological mechanism is compromised in patients with SLE. Establishing mice with either conditional knockout (cKO) or knockin (cKI) of the *E4bp4* gene in T cells reveals that E4BP4 strongly inhibits Tfh cell differentiation. Mechanistically, E4BP4 regulates *Bcl6* transcription by recruiting the repressive epigenetic modifiers HDAC1 and EZH2. E4BP4 phosphorylation site mutants have limited capability with regard to inhibiting Tfh cell differentiation. In SLE, we detected impaired phosphorylation of E4BP4, finding that this compromised transcription factor is positively correlated with disease activity. These findings unveiled molecular mechanisms by which E4BP4 restrains Tfh cell differentiation, whose compromised function is associated with uncontrolled autoimmune reactions in SLE.**

## Introduction

T follicular helper (Tfh) cells are a subset of specialized effector $CD4^+$ T cells mediating B cell selection, proliferation, and differentiation in germinal centers (GCs) (1). Aberrant activation of these cells can disturb GC selection and enable autoreactive antibody production with the potential to induce autoimmune diseases in mouse models (2, 3). Increased generation of Tfh cells is also a common feature in patients with autoimmune diseases (4, 5) such as systemic lupus erythematosus (SLE), a long-term autoimmune disease. SLE patients exhibit enhanced GC formation, which contributes to the generation of autoantibodies, which in turn cause inflammation in connective tissues.

Many studies involving SLE, including a previous one published by our group, have demonstrated that circulating Tfh (cTfh) cells in peripheral blood mononuclear cells (PBMCs) show an increase in number and are positively correlated with autoantibody titers and disease progression (6–8). This result indicates that therapeutic targeting of Tfh cells could constitute a feasible approach with regard to reinstating immune tolerance for treatment of autoimmune diseases. T follicular regulatory (Tfr) cells constitute a recently described subpopulation of follicular T cells that limit the frequency of self-reactive T cell and B cell responses in the GCs (9–15). Recent studies have shown that, as opposed to the absolute numbers of cell types, it is the ratio of Tfr to Tfh in the GCs that correlates with suppression of antibody responses and autoantibody-mediated autoimmune diseases (13, 16, 17).

Tfh cells express a set of featured markers, such as chemokine receptor 5 (CXCR5), inducible T cell costimulator (ICOS), programmed cell death 1 (PD-1), and B-helper cytokine interleukin-21 (IL-21) (2). Differentiation of Tfh cells is regulated by extracellular signals from antigens; stimulatory or inhibitory coreceptors including ICOS, PD-1, CD40L, and OX40; and cytokines including IL-6 and IL-21 (18). Downstream of these factors, dozens of transcription factors, RNA-binding proteins, and microRNAs have been reported to control the gene expression specification for Tfh cell differentiation (19–21). Among these, the transcription factor BCL6 is considered to constitute a master regulator due to the fact that it is necessary with regard to driving the differentiation of Tfh cells (19, 22). Nonetheless, the mechanisms underlying the tuning of Bcl6 expression remain poorly understood.

E4BP4 is a mammalian basic leucine zipper transcription factor with a repression domain of a 65–amino acid segment near the C-terminus of the polypeptide (23). The role played by E4BP4 in the immune system is starting to emerge. It is vital in IL-4–induced GLε transcription in IgE class switching (24), and is also essential for NK cell generation, development, maturation, and function (25, 26). In T cell subsets, E4BP4 regulates the plasticity of cytokine productions in Th1, Th2, Treg, and NKT cells (27, 28). In addition, E4BP4 regulates Th17 cell development in a circadian manner by targeting the transcription factor REV-ERBα (29). Overexpression

**Authorship note:** ZW and MZ are co–first authors and they contributed equally to this work.
**Conflict of interest:** The authors have declared that no conflict of interest exists.

**Submitted:** March 22, 2019; **Accepted:** March 17, 2020; **Published:** June 2, 2020.
**Reference information:** *J Clin Invest*. 2020;130(7):3717–3733.
https://doi.org/10.1172/JCI129018.

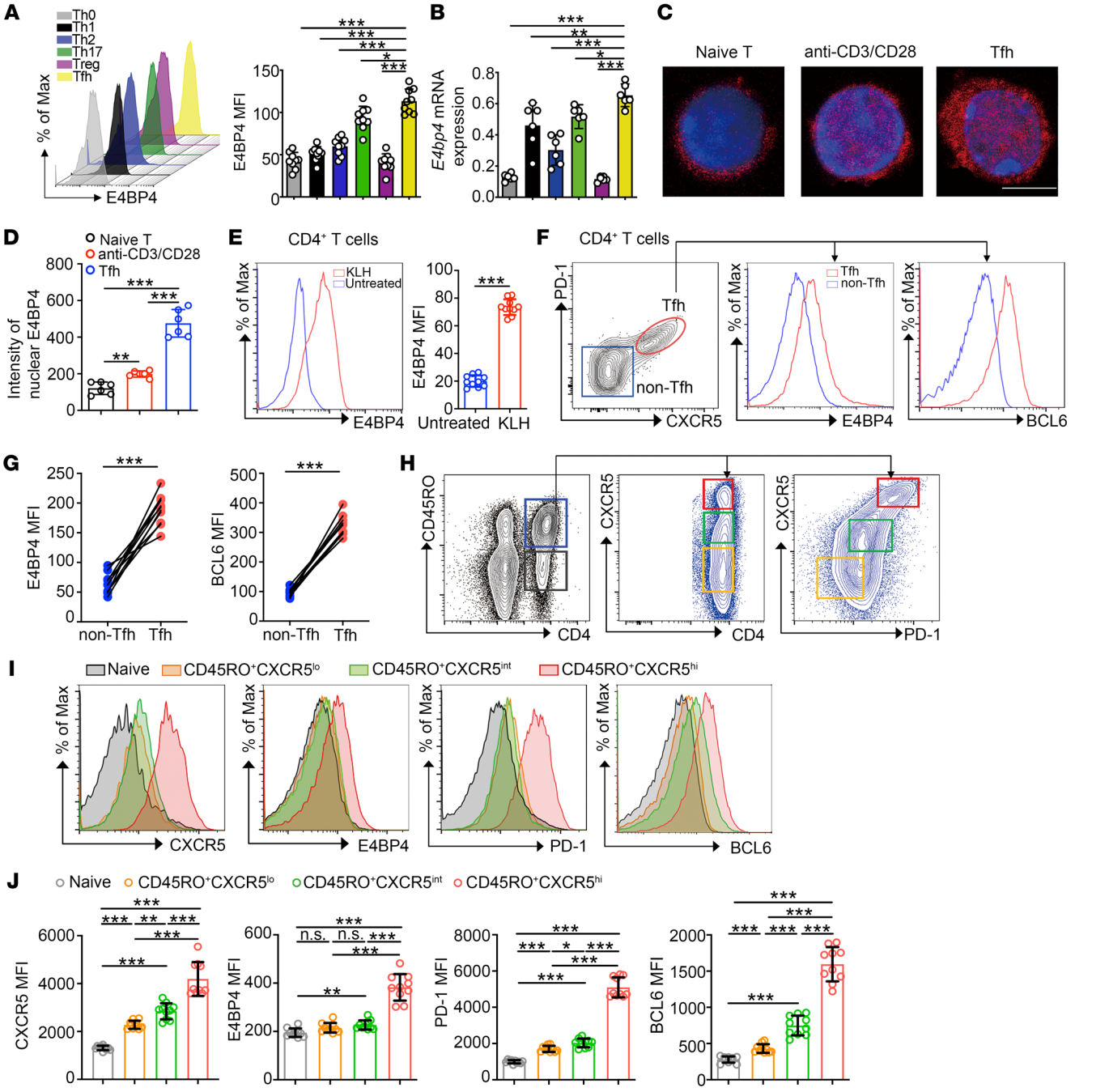


**Figure 1. E4BP4 is more abundantly expressed in Tfh cells.** (**A**) Analysis of naive CD4+ T cells from 8-week-old C57BL/6 mice stimulated in vitro under Th0, Th1, Th2, Th17, Treg, and Tfh cell–polarizing conditions for 3 days (Th0, Th1, Th17, Treg, and Tfh cells) or 5 days (Th2 cells) by flow cytometry for mean fluorescence intensity (MFI) of E4BP4 ($n$ = 9). (**B**) mRNA expression of *E4bp4* in T cell subsets indicated in **A** ($n$ = 6). (**C**) Naive CD4+ T cells, anti-CD3/CD28–activated CD4+ T cells, and in vitro–polarized Tfh cells were stained by anti-E4BP4 (red) and DAPI (blue) and analyzed by confocal microscopy. Scale bar: 5 μm. (**D**) Statistical intensity of E4BP4 in nuclei ($n$ = 6). (**E**) Flow cytometric analysis of E4BP4 expression in mice CD4+ T cells ($n$ = 10). (**F**) Gating strategy of CXCR5+PD-1+(Tfh) or CXCR5−PD-1− (non-Tfh) cell phenotype in CD4+ T cells from KLH immunized C57BL/6 mice. Analysis of E4BP4 and BCL6 expression (MFI) is shown in the right panel. (**G**) Statistical analysis of **F** ($n$ = 10). (**H**) Gating strategy of human tonsillar CD45RO+ memory/effector or CD45RO− naive CD4+ T cells. CD45RO+ cells were subsequently divided into CXCR5lo, CXCR5int, and CXCR5hi gates. (**I** and **J**) Representative histograms of CXCR5, BCL6, PD-1, and E4BP4 MFI expressions in subsets outlined in **H** ($n$ = 10). Data are representative of 3 independent experiments. For **A**, **B**, **D**, and **J**, 1-way ANOVA with Dunnett's post hoc test, **E** and **G** with Student's $t$ test. *$P$ < 0.05; **$P$ < 0.01; ***$P$ < 0.001.

of E4BP4 in Treg cells results in decreased expression of FoxP3 and other Treg signature genes (30). Despite the significant roles played by E4BP4 in immune cell development and function, its role in relation to Tfh cells has not yet been reported.

In the present study, E4BP4 was observed to be highly expressed in Tfh cells in both mice and humans, and ablation of E4BP4 in CD4+ T cells resulted in augmented GC reactions upon immunization. At the molecular level, we provided evidence that

E4BP4 recruits histone methyltransferase EZH2 and deacetylase HDAC1 to the *Bcl6* gene promoter. Mutant E4BP4 lacking serine phosphorylation sites reduced E4BP4-mediated inhibition of Tfh cell differentiation. Patients with SLE display an increase in total E4BP4 but a decrease in phosphorylated E4BP4. The compromised E4BP4 was positively correlated with disease activity. In summary, our results unveil the critical role of E4BP4 in regulating humoral immunity and autoimmune responses. Malfunction of E4BP4 will give rise to excessive Tfh cell accumulation in SLE.

## Results

*E4BP4 is highly expressed and activated in follicular T cells*. To establish the pattern of expression of endogenous E4BP4 in different $CD4^+$ T subsets, naive $CD4^+$ T cells from C57BL/6 mice were stimulated under different Th subset–polarizing (Th0, Th1, Th2, Th17, Treg, and Tfh) conditions. Both E4BP4 protein and mRNA expression levels were determined. The Tfh cells presented an extremely high expression of E4BP4 as compared with their expression in other Th subsets (Figure 1, A and B). We then examined a group of cytokines to observe the manner in which E4BP4 expression changes under different conditions. E4BP4 displayed a relatively higher expression after treatment with IL-21 or IL-6 in $CD4^+$ T cells (Supplemental Figure 1; supplemental material available online with this article; https://doi.org/10.1172/JCI129018DS1). This was also reflected with the nuclear expression of E4BP4, in which staining of E4BP4 protein by immunofluorescence appeared to be stronger in anti-CD3/CD28–activated $CD4^+$ T cells and in Tfh cells (in vitro–polarized) than in naive $CD4^+$ T cells (Figure 1, C and D).

Subsequently, we sought to address the expression of E4BP4 in Tfh cells from immunized animal models. We analyzed cells from keyhole limpet hemocyanin–immunized (KLH-immunized) or sheep red blood cell–immunized (SRBC-immunized) C57BL/6 mice. We observed increased expression of E4BP4 in $CD4^+$ T cells following KLH immunization (Figure 1E). We then compared E4BP4 and BCL6 expression in $CD4^+CXCR5^+PD\text{-}1^+$ Tfh cells and $CD4^+CXCR5^-PD\text{-}1^-$ non–Tfh cells from KLH- and SRBC-immunized mice. The Tfh cell population exhibited a higher amount of both E4BP4 and BCL6 than the non–Tfh cells (Figure 1, F and G, and Supplemental Figure 2A). In addition, we found that E4BP4 expression in $FoxP3^+$ Tfr cells decreased as compared with its expression in $CD4^+CXCR5^+PD\text{-}1^+$ Tfh cells in immunized C57BL/6 mice, which implies that E4BP4 is more highly expressed in $FoxP3^-$ Tfh cells (Supplemental Figure 2B).

We further characterized E4BP4 expression in human T cells. E4BP4 protein expression was upregulated in anti-CD3/CD28–activated $CD4^+$ T cells (Supplemental Figure 3A). In addition, E4BP4 was increasingly expressed during Tfh cell differentiation (Supplemental Figure 3B). In human tonsillar $CD4^+$ T helper subsets, E4BP4 was highly expressed in Tfh cells (Supplemental Figure 3, C and D). We observed a notably high E4BP4 expression in $CD4^+CD45RO^+CXCR5^{hi}$ Tfh cells along with an increase in CXCR5, PD-1, and BCL6 (Figure 1, H–J). E4BP4 expression was positively correlated with CXCR5, PD-1, and BCL6 (Supplemental Figure 3E). In summary, these data revealed that E4BP4 was highly expressed in both mice and human Tfh cells.

*Increased population of Tfh cells in E4bp4-cKO mice*. The increased expression of E4BP4 in Tfh cells prompted us to investigate whether E4BP4 deficiency would give rise to a phenotypical abnormality. To this end, we used mice with conditional knockout of *E4bp4* in T cells (*E4bp4*-cKO) (ref. 27 and Supplemental Figure 4A). In comparison with the WT control, the *E4bp4*-cKO mice exhibited an altered ratio of the $CD4^+$ and $CD8^+$ T cell populations, as seen in the increase in $CD8^+$ T cells and the decrease in $CD4^+$ T cells in lymph nodes and spleens (Figure 2A). The *E4bp4*-cKO mice adopted a memory-like phenotype, as witnessed by a slight increase in the population of $CD44^{hi}CD62L^{lo}$ effector memory (EM) cells in lymph nodes in both $CD4^+$ and $CD8^+$ T cells compared with their littermate controls (Figure 2, B and C). These data suggest that T cells from *E4bp4*-cKO mice show a preferential expression of activated phenotypes as compared with their WT littermates.

We then examined the percentages of $FoxP3^+$ Treg, $CD4^+CXCR5^+PD\text{-}1^+$ Tfh cells, and $FoxP3^+$ Tfr cells in unimmunized *E4bp4*-cKO mice and their littermate controls. The frequency of Treg cells showed a slight increase in the *E4bp4*-cKO mice; however, we observed a proportional decrease in Tfr cells in total $CD4^+CXCR5^+PD\text{-}1^+$ Tfh cells (Figure 2, D and E). The loss of Tfr cells was accompanied by an increase in Tfh cells in the *E4bp4*-cKO mice, as compared with their WT littermates (Figure 2F). Thus, despite the increased expression of FoxP3 in total $CD4^+$ T cells, FoxP3 expression in Tfh cells declined, suggesting a poor capacity to suppress antibody production in the *E4bp4*-cKO mice.

*Loss of E4BP4 in $CD4^+$ T cells enhances differentiation of Tfh-like cells in vitro*. We then investigated the role of E4BP4 in regulating Tfh cell differentiation in vitro. CXCR5 and PD-1 were stained in naive $CD4^+$ T cells as a negative control (Figure 3, A and B). Naive $CD4^+$ T cells were cultured in vitro under Tfh-polarizing conditions (31) for 5 days. The expressions of CXCR5 and PD-1 were enhanced in the $CD4^+$ T population with E4BP4 deficiency, along with enhanced protein levels of BCL6 and IL-21 in the $CD4^+CXCR5^+PD\text{-}1^+$ Tfh-like population as compared with their WT littermates (Figure 3, C and D). Moreover, we constructed an *E4bp4* conditional knockin mouse (*E4bp4*-cKI), which specifically overexpresses E4BP4 in T cells (Supplemental Figure 4B). *E4bp4*-cKI naive $CD4^+$ T cells appeared to abolish their differentiation of $CD4^+CXCR5^+PD\text{-}1^+$ Tfh-like cells, and had lower protein levels of BCL6 and IL-21, as compared with their WT littermates (Figure 3, E and F). These data indicated that E4BP4 is a negative regulator of Tfh cell differentiation. We conducted an in vitro Tfh coculture experiment which demonstrated that the ability of E4BP4-deficient Tfh cells to promote IgG1 secretion was similar to that of the WT mice (Supplemental Figure 5, A and B). This implies that Tfh cell function is independent from E4BP4 regulation. In addition, we explored the potential role of E4BP4 in regulating other $CD4^+$ Th subsets. The results showed that E4BP4 exhibited an inhibitory role in Th17 and Treg cell differentiation but revealed no regulatory roles in Th1 and Th2 cell differentiation (Supplemental Figure 6, A–C).

To confirm that the in vitro–polarized Tfh-like cells from the *E4bp4*-cKO mice presented features of Tfh cells, we performed RNA sequencing (RNA-seq) to determine the global transcriptomic profile of the *E4bp4*-cKO Tfh-like cells. Comparison of the gene expression profile of Tfh-like cells and the published data set (GEO GSE16697), which exhibited genes that showed an increase in Tfh cells in relation to non–Tfh cells for gene set

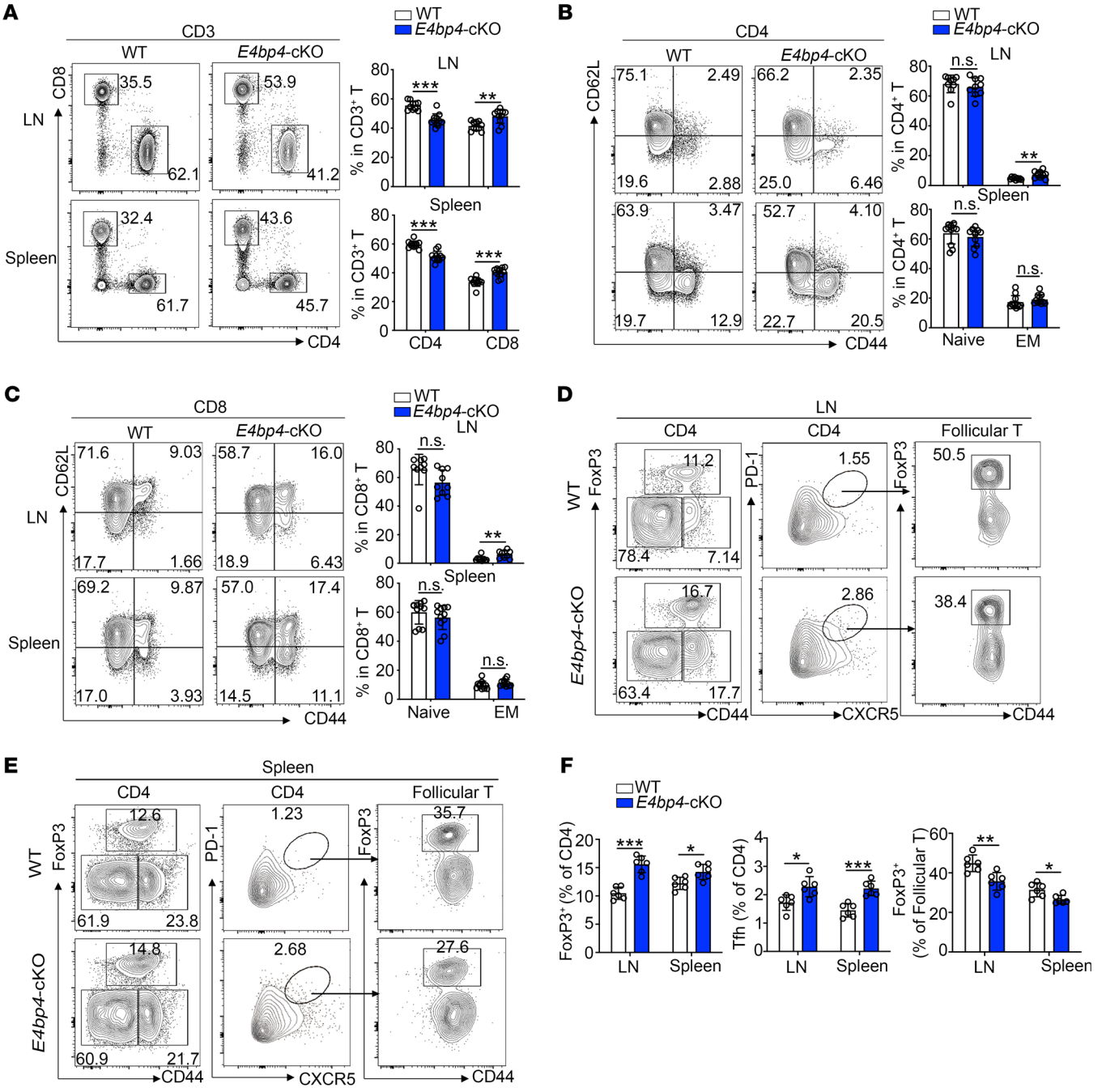


**Figure 2. Phenotypical analysis of the *E4bp4*-cKO mice.** (**A**) Flow cytometric analysis of the CD4$^+$ and CD8$^+$ T cell populations in CD3$^+$ T cells of nonimmunized WT and *E4bp4*-cKO mice. Statistical analysis is shown on the right. (**B** and **C**) Flow cytometric analysis of CD44$^+$ and CD62L$^+$ cells in CD4$^+$ and CD8$^+$ T cell populations ($n$ = 10). (**D** and **E**) Flow cytometric analysis of Treg, Tfh, and Tfr cells. (**F**) Statistical analysis of **D** and **E** ($n$ = 6). Data are representative of 4 independent experiments. LN, lymph node; EM, effector memory. Student's $t$ test. *$P$ < 0.05; **$P$ < 0.01; ***$P$ < 0.001.

enrichment analysis (GSEA), revealed that the characteristic in *E4bp4*-cKO Tfh-like cells was consistent with the expression of Tfh cell signature genes (Figure 3G). Herein we found differential expression of 5161 genes by comparing the WT and *E4bp4*-cKO Tfh-like cells (Figure 3H). Of these differentially expressed genes, 2661 were downregulated (Supplemental Table 1) and 2500 were upregulated (Supplemental Table 2) in *E4bp4*-cKO Tfh-like cells relative to their expression in the WT Tfh-like cells. Several Tfh signature genes, such as *Bcl6*, *Il21*, *Pdcd1*, *Tcf7*, *Pou2af1*, *Cd40lg*, and *Tiam1,* increased in the *E4bp4*-cKO Tfh-like cells, whereas *Prdm1* and *Stat5b* decreased in the *E4bp4*-cKO Tfh-like cells (Figure 3I). Genes associated with Tfr cells were reduced in *E4bp4*-cKO Tfh-like cells (Figure 3J), such as *FoxP3*, *Il10*, and *Ctla4*. We further confirmed these gene expressions by quantitative RT-PCR (Supplemental Figure 7, A–J). Collectively, these data indicate that E4BP4 regulates the expression of multiple genes crucially involved in Tfh and Tfr cell differentiation.

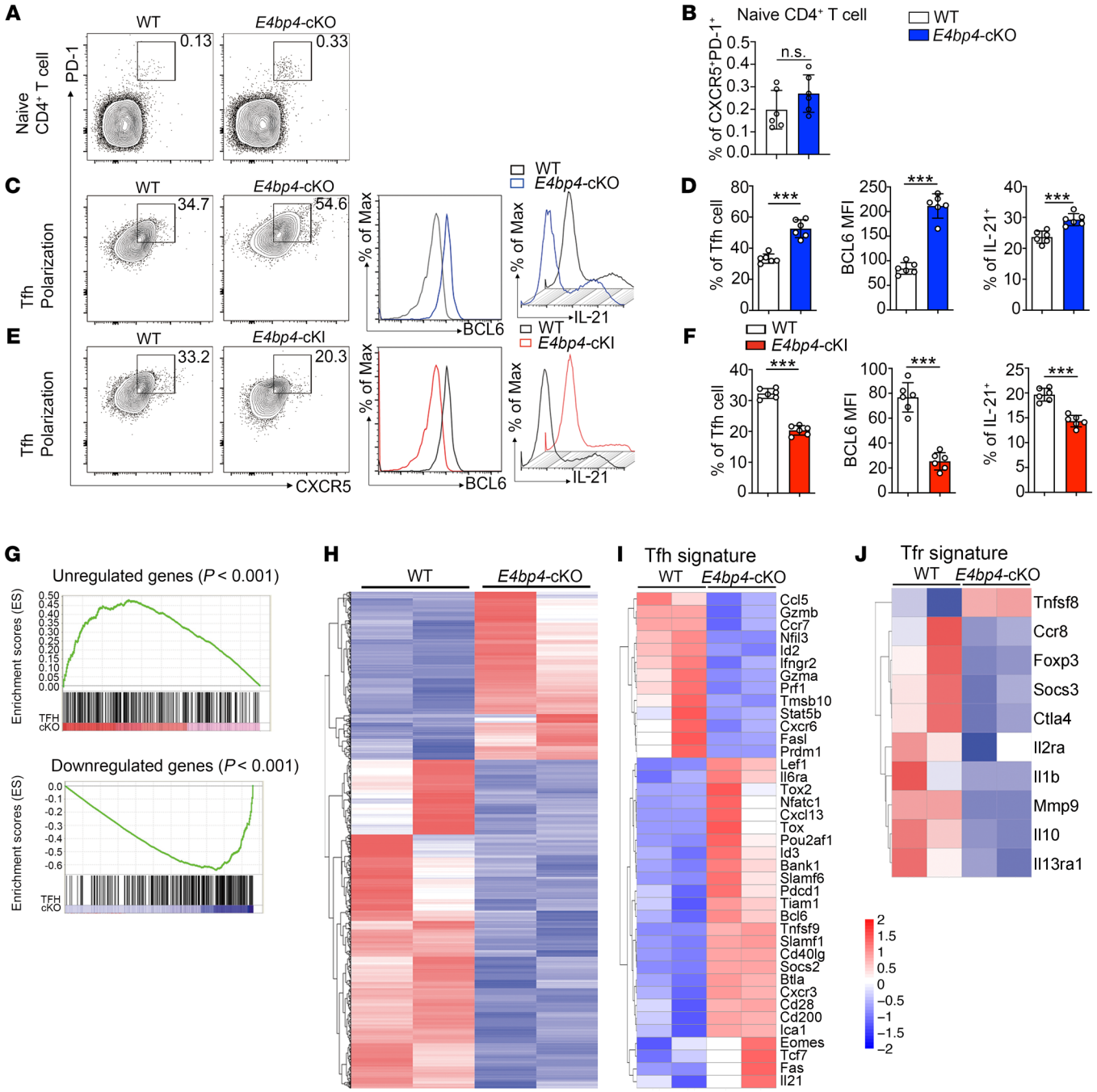


**Figure 3. E4BP4 regulates Tfh cell differentiation in vitro.** (**A**) Flow cytometric analysis of CXCR5$^+$PD-1$^+$ in naive CD4$^+$ T cells from the *E4bp4*-cKO and WT mice. Statistical analysis is indicated in **B**. (**C**–**F**) Flow cytometric analysis of in vitro–polarized Tfh-like cells from the *E4bp4*-cKO and WT mice and from the *E4bp4*-cKI and WT mice. Representative histograms of BCL6 and IL-21 expression in CD4$^+$CXCR5$^+$PD-1$^+$ Tfh-like cells are shown in **D** and **F** ($n$ = 6). (**G**) Gene set enrichment analysis of gene signatures (either upregulation or downregulation) in Tfh cells relative to their expression in non–Tfh cells from published data (GEO accession code GSE16697), and differentially expressed genes between the in vitro–polarized *E4bp4*-cKO Tfh-like cells and WT Tfh-like cells. Red/blue rectangles indicate enriched genes in the *E4bp4*-cKO Tfh-like cells. (**H**) RNA-seq analysis of gene expression of in vitro–polarized Tfh-like cells; colors indicate upregulated (red) or downregulated (blue) genes. (**I**) Clustered heatmap of 39 Tfh signature genes regulated by E4BP4. (**J**) Clustered heatmap of 10 Tfr signature genes regulated by E4BP4. The data were normalized from 2 replicates ($n$ = 2). Genes with the most transcriptional changes are listed. (**A**–**F**) Data are representative of 3 independent experiments. Student's $t$ test. *$P$ < 0.05; **$P$ < 0.01; ***$P$ < 0.001.

*Deletion of E4bp4 in CD4$^+$ T cells provokes an augmented GC reaction*. Subsequently, we examined whether E4BP4 plays a functional role in GC responses upon immunization. We first detected the percentage of CD4$^+$ and CD8$^+$ T cells in *E4bp4*-cKO mice, and found a slight increase in CD8$^+$ T cells (Supplemental Figure 8, A and B). We observed higher percentages of Treg cells and Tfh cells, as well as a proportional decrease in FoxP3$^+$ Tfr cells in follicular T cells (Figure 4, A and B). In addition, we

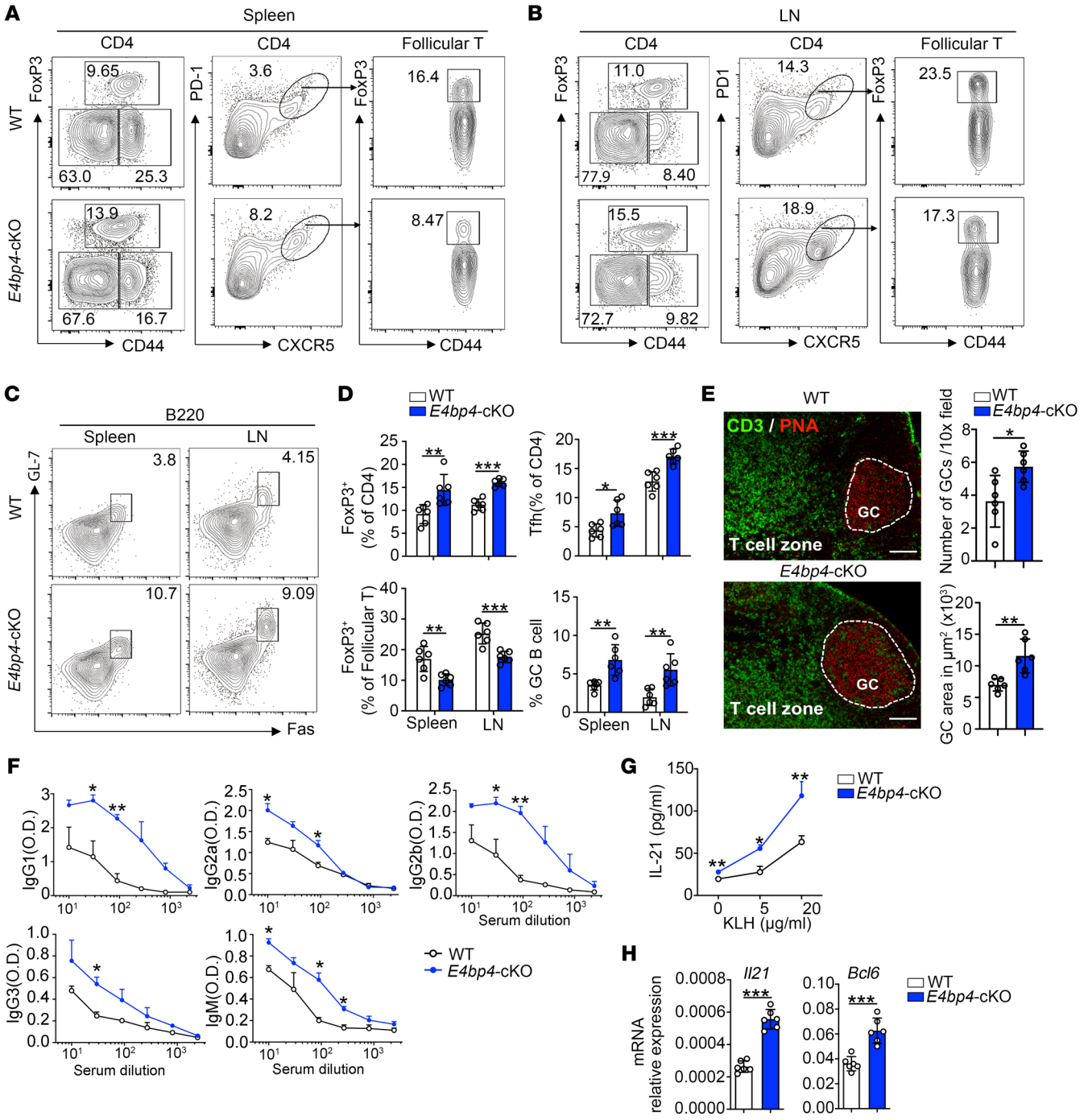


**Figure 4. E4BP4 deficiency promotes antigen-specific GC responses.** Age-matched WT or *E4bp4*-cKO mice were immunized with KLH for 14 days, then lymph node and spleen cells were harvested. (**A** and **B**) Flow cytometric analysis of FoxP3$^+$ Treg cells, CD4$^+$CXCR5$^+$PD-1$^+$ Tfh cells, and FoxP3$^+$ Tfr cells in follicular T cells. (**C**) Analysis of B220$^+$Fas$^+$GL-7$^+$ GC B cells. (**D**) Summary of the percentage of FoxP3$^+$ Treg cells, Tfh cells, and FoxP3$^+$ Tfr cells in follicular T cells, as described in **A** and **B**, and GC B cells, as described in **C**. (**E**) Immunofluorescence of GCs from WT and *E4bp4*-cKO mice, representative images of CD3 and PNA staining of LNs. Scale bars: 200 μm. Quantification of PNA$^+$ GC areas and number of PNA$^+$ follicles per lymph node. (**F**) Detection of serum anti-KLH–specific IgG1, IgG2a, IgG2b, IgG3, and IgM by ELISA. (**G**) Draining lymph node cells were restimulated with KLH for 3 days, and supernatant IL-21 expression was detected by ELISA. (**H**) *Il21* and *Bcl6* mRNA expression levels were analyzed by qPCR ($n$ = 6). Data are representative of 4 independent experiments. Student's $t$ test. *$P$ < 0.05; **$P$ < 0.01; ***$P$ < 0.001.

observed a higher percentage of B220$^+$Fas$^+$GL7$^+$GC B cells in the *E4bp4*-cKO mice (Figure 4, C and D). PNA staining of histological sections revealed a pronounced GC response (Figure 4E). Consecutively, serum KLH-specific Abs IgM and class-switched IgG1, IgG2a, IgG2b, and IgG3 titers increased in the *E4bp4*-cKO mice compared with their WT controls (Figure 4F). However, we found that the affinity maturation of serum IgG1 Ab did not appear to show a significant difference between the *E4bp4*-cKO

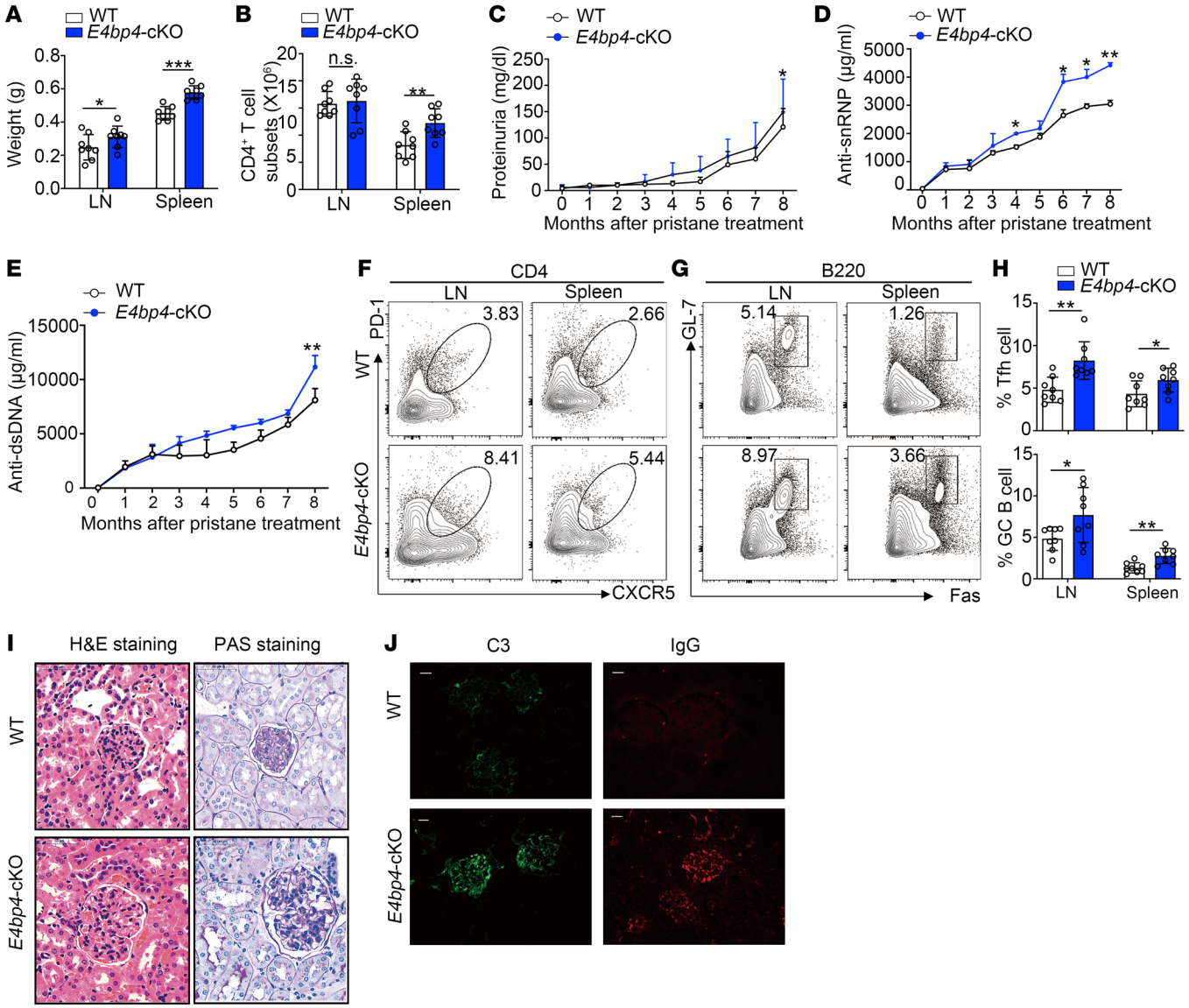


**Figure 5. E4BP4 deficiency exacerbates pristane-induced lupus-like diseases.** Age-matched WT and *E4bp4*-cKO mice were administered pristane. After 32 weeks, the mice were sacrificed for the development of autoimmune traits. (**A**) The spleens and lymph nodes were weighed. (**B**) The number of $CD4^+$ T cells from splenocytes and lymphocytes was estimated. (**C**) The level of proteinuria was measured by ELISA. (**D** and **E**) Serum anti-snRNP and anti-dsDNA antibodies were measured by ELISA. Flow cytometric analysis of (**F**) Tfh cells ($CD4^+$ $CXCR5^+PD\text{-}1^+$) and (**G**) GC B cells ($B220^+GL\text{-}7^+FAS^+$). (**H**) Statistical analysis of **F** and **G**. (**I**) Representative images of H&E- or PAS-stained kidney sections were collected at the end of the observation period. Scale bars: 50 μm. (**J**) C3 and IgG deposition in the kidney sections were assessed by immunofluorescence staining. Scale bars: 25 μm ($n$ = 8). Data are representative of 2 to 3 independent experiments. Student's $t$ test. $^*P < 0.05$; $^{**}P < 0.01$; $^{***}P < 0.001$.

and the WT mice, although the *E4bp4*-cKO mice produced more $NP_2$- and $NP_{27}$-specific IgG1 than their WT littermates (Supplemental Figure 9, A–C). In order to evaluate memory responses, lymphocytes from the *E4bp4*-cKO and WT mice were restimulated with KLH to examine the regulatory effect of E4BP4. Lymphocytes from the *E4bp4*-cKO mice secreted more soluble IL-21 (Figure 4G), and expressed higher levels of *Bcl6* and *Il21* mRNAs (Figure 4H) in comparison with their WT littermates. The augmented GC responses in the *E4bp4*-cKO mice compared with their littermate controls were independent from the type and strength of immunization, as demonstrated by SRBC immunization (Supplemental Figure 10, A and B).

To investigate whether E4BP4 regulates Tfh cell differentiation in a cell-intrinsic manner, naive $CD4^+$ T cells from WT or *E4bp4*-KO (Supplemental Figure 4C) together with WT B cells were transferred into *Rag2*$^{-/-}$ recipient mice, following immunization with KLH (Supplemental Figure 11A). The overall GC responses in the *Rag2*$^{-/-}$ mice that received *E4bp4*-KO naive $CD4^+$T cells were enhanced as compared with those in the *Rag2*$^{-/-}$ mice that received WT donor cells (Supplemental Figure 11, B–E).

As a complementary approach, we evaluated the effect of E4BP4 overexpression on Tfh cell differentiation. Upon immunization with KLH or SRBCs, the *E4bp4*-cKI mice presented a reduced GC response as compared with their WT littermates (Supplemental

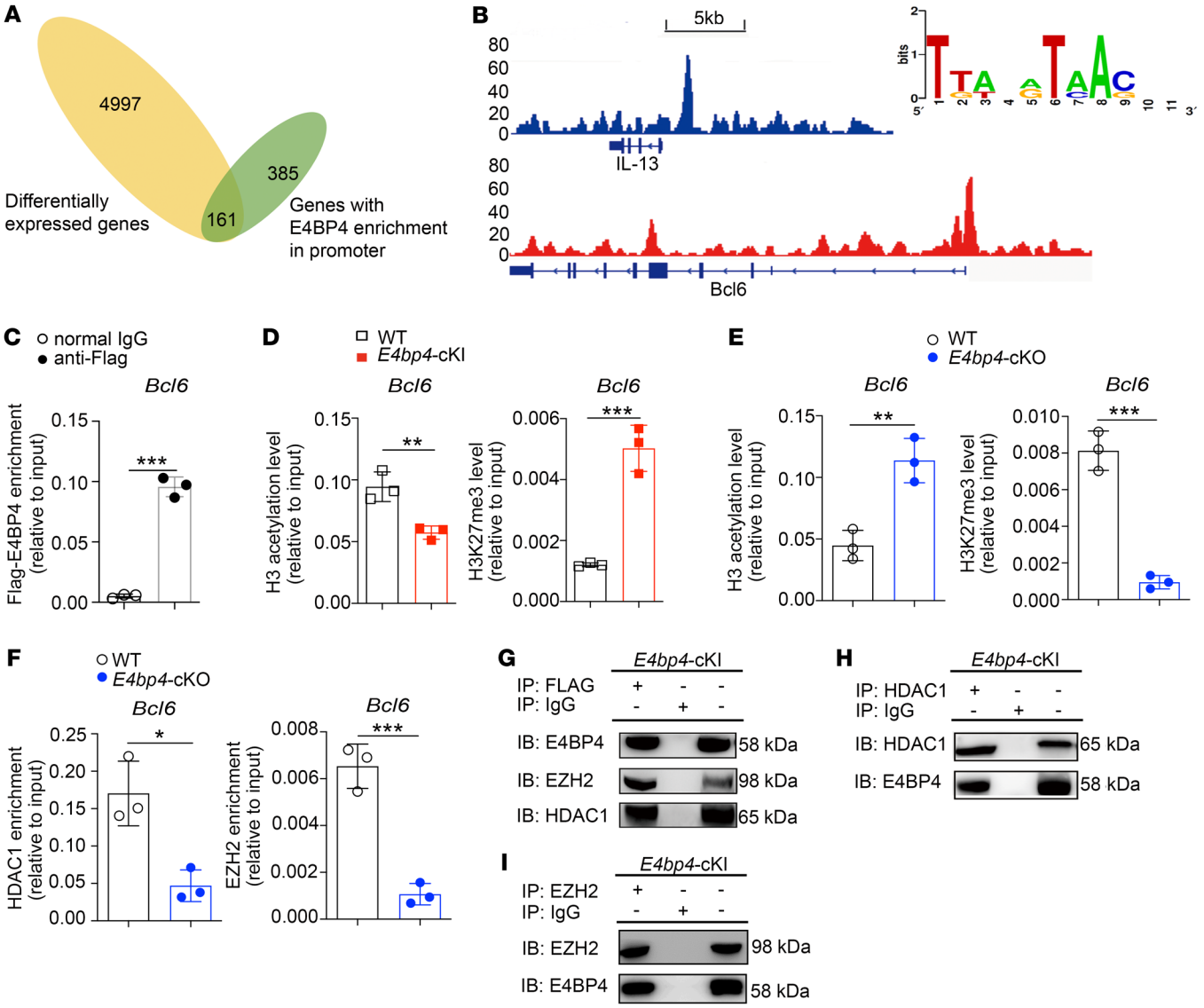


**Figure 6. E4BP4 regulates Tfh cell differentiation by binding to the *Bcl6* promoter.** (**A**) Venn diagram showing the overlap between the genes with E4BP4 enrichment in promoter (green) and differentially expressed genes revealed by expression profile analysis (yellow). (**B**) ChIP-Seq analysis of E4BP4-binding peaks located at gene loci *Bcl6* and *Il13* in the *E4bp4*-cKI CD4$^+$ T cells. The Bcl6-binding site motif is shown (right). (**C**–**F**) *E4bp4*-cKI/*E4bp4*-cKO naive CD4$^+$ T cells were cultured under Tfh-polarizing conditions for 5 days. (**C**) ChIP-PCR was performed with IgG and anti-FLAG antibody to analyze the binding activity of E4BP4 to *Bcl6*. (**D**) The H3 acetylation and H3K27 trimethylation levels in the *Bcl6* promoter region in WT versus *E4bp4*-cKI mice are shown. (**E**) The H3 acetylation and H3K27 trimethylation levels in the *Bcl6* promoter region in WT versus *E4bp4*-cKO mice are shown. (**F**) The enrichments of HDAC1 and EZH2 in the *Bcl6* promoter region in WT versus *E4bp4*-cKO mice are shown ($n$ = 3). (**G**–**I**) Anti-FLAG antibody, anti-HDAC1, and anti-EZH2 antibodies were used for coimmunoprecipitation experiments to analyze the interaction between E4BP4 and HDAC1 or EZH2 in *E4bp4*-cKI Tfh-like cells. Each result corresponds to data pooled from 3 independent experiments. Student's $t$ test. ***$P$ < 0.001; **$P$ < 0.01; *$P$ < 0.05.

Figure 12, A–D, and Supplemental Figure 13, A and B). In summary, these results are consistent with the hypothesis that E4BP4 exerts negative regulatory effects upon Tfh cell differentiation.

*E4BP4 deficiency gives rise to an aggravated humoral autoimmune response*. In order to determine how E4BP4 affects Tfh cell differentiation in autoimmune conditions, we performed immunization with pristane, which causes lupus-like disease in mice (32, 33). At the end of the observation period, we observed increased weights and higher CD4$^+$ T cell numbers in the spleen and lymph nodes of the *E4bp4*-cKO mice (Figure 5, A and B). The results of the urinalysis revealed a slight increase in proteinuria level in the *E4bp4*-cKO mice as compared with that of the WT mice (Figure 5C). The serum levels of the anti-snRNP and anti-dsDNA antibodies in the *E4bp4*-cKO mice showed significant increases (Figure 5, D and E). Flow cytometry analysis showed an increase in CD4$^+$CXCR5$^+$PD-1$^+$ Tfh cells and B220$^+$Fas$^+$GL7$^+$ GC B cells in the *E4bp4*-cKO mice as compared with the WT mice (Figure 5, F–H). Hematoxylin and eosin (H&E) and PAS staining of kidney sections exhibited a much higher amount of pathological lesions of the glomerulus in the *E4bp4*-cKO mice as compared with that of the WT mice (Figure 5I). Immunoglobulin and complement detection revealed a

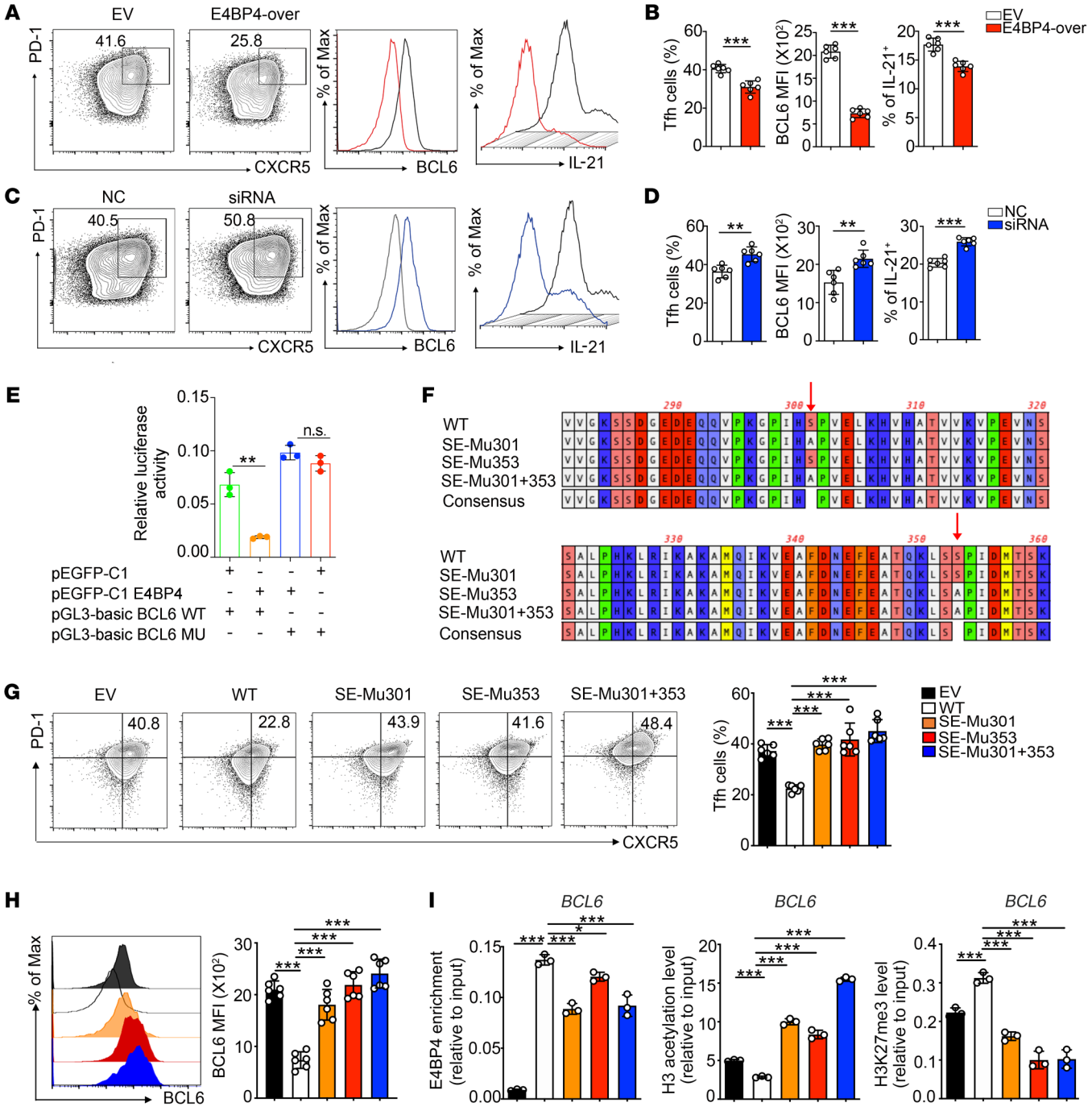


**Figure 7. Phosphorylation-defective mutant of E4BP4 promotes human Tfh cell differentiation.** (**A**–**D**) CD4⁺ T cells isolated from healthy donors were transfected with E4BP4 overexpression (E4BP4-over) plasmid or empty vector (EV), as well as with E4BP4 siRNA and negative control (NC). The cells were then cultured under Tfh polarization conditions for 5 days. (**A**) Flow cytometric analysis of CD4⁺CXCR5⁺PD-1⁺ Tfh cells in EV and E4BP4-over group. Representative histograms of BCL6 and IL-21 expressions in CD4⁺CXCR5⁺PD-1⁺ Tfh cells are shown on the right. (**B**) Statistical analysis of **A**. (**C**) Analysis of CD4⁺CXCR5⁺PD-1⁺ Tfh cells in NC and siRNA groups. Representative histograms of BCL6 and IL-21 expressions in CD4⁺CXCR5⁺PD-1⁺ Tfh cells are shown. (**D**) Statistical analysis of **C** ($n$ = 6). (**E**) The luciferase reporter assay in HEK293T cells by electroporation with the reporter plasmids pEGFP-C1 empty vector plus pGL3-basic BCL6 WT or pEGFP-C1 E4BP4 plus pGL3-basic BCL6 WT or pEGFP-C1 E4BP4 plasmid plus pGL3-basic BCL6 mutant or pEGFP-C1 empty vector plasmid plus pGL3-basic BCL6 mutant ($n$ = 3). (**F**) Phosphomimetic mutation of E4BP4 putative serine sites at ser301 or ser353 mutants or double mutants (S to A). (**G**) Mutant and WT versions of E4BP4 were expressed in human CD4⁺ T cells, separately. Cells were then cultured under Tfh-polarizing conditions for 5 days and the percentage of CD4⁺CXCR5⁺PD-1⁺ Tfh cells was analyzed by flow cytometry. (**H**) BCL6 MFI expression in CD4⁺CXCR5⁺PD-1⁺ Tfh cells indicated in **G** was analyzed by flow cytometry ($n$ = 6). (**I**) Mutant and WT versions of E4BP4 were expressed in Jurkat cells. ChIP-PCR was used to detect levels of E4BP4 enrichment, H3 acetylation, and H3K27 trimethylation in the *BCL6* gene promoter ($n$ = 3). Data are representative of 3 independent experiments. For **B**, **D**, and **E**, Student's $t$ tests were used. For **G**–**I**, 1-way ANOVA analysis with Dunnett's post hoc test was used. *$P$ < 0.05; **$P$ < 0.01; ***$P$ < 0.001.

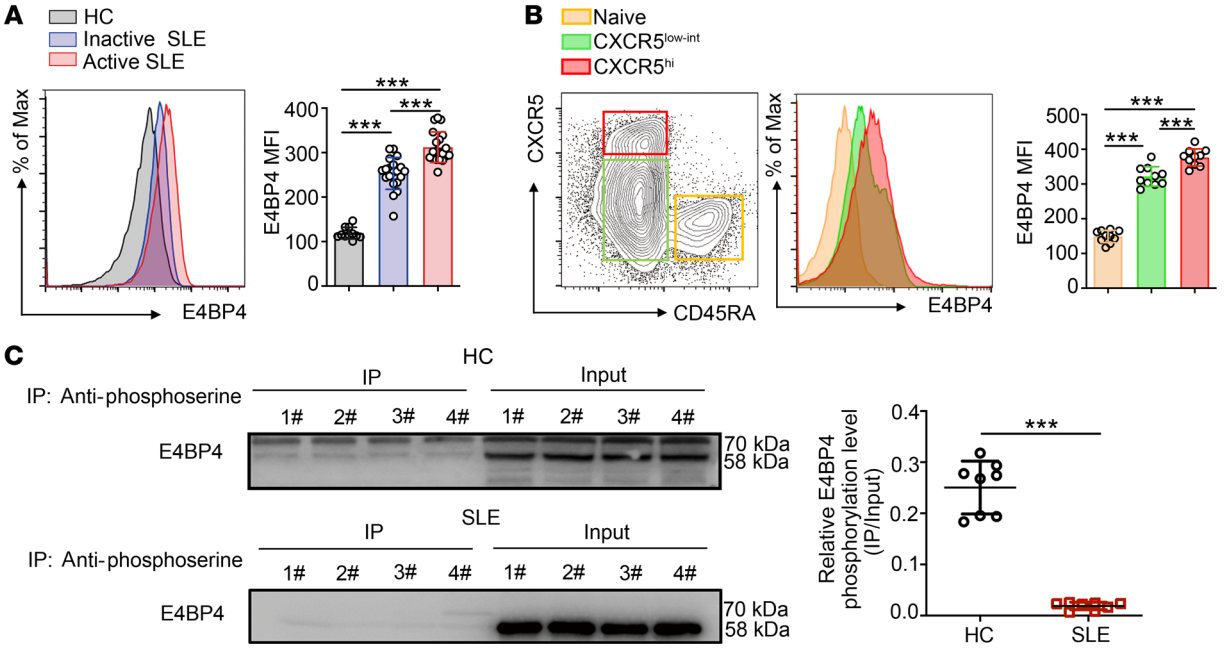


**Figure 8. Defective phosphorylation of E4BP4 in SLE.** (**A**) Analysis of E4BP4 MFI expression in CD4$^+$ T cells in healthy subjects ($n$ = 11), inactive SLE patients ($n$ = 20), and active SLE patients ($n$ = 20) by flow cytometry. (**B**) Gating strategy of SLE PBMC CD45RA$^+$, CD45RA$^-$CXCR5$^{lo}$, and CD45RA$^-$CXCR5$^{hi}$ subsets in CD4$^+$ T cells. Analysis of E4BP4 MFI expression in indicated subsets was shown (right) by flow cytometry. Dots indicate individual donors ($n$ = 10). (**C**) Immunoprecipitating with antiphosphoserine antibody before Western blot analysis of anti-E4BP4 in SLE CD4$^+$ T and NC CD4$^+$ T cells ($n$ = 8). Representative results of Western blot analysis (IP/Input) are shown (right). Data are representative of 3 independent experiments. For **A** and **B**, 1-way ANOVA with Tukey's test was used. For **C**, Student's $t$ test was used. *$P$ < 0.05; **$P$ < 0.01; ***$P$ < 0.001.

severe lupus-like phenotype in the glomeruli of the *E4bp4*-cKO mice (Figure 5J). Thus, *E4bp4* deficiency in T cells exacerbates humoral autoimmunity.

*E4BP4 directly modulates Bcl6 expression via epigenetic mechanisms*. To identify gene loci enriched by E4BP4, a ChIP-seq assay was performed in the *E4bp4*-cKI CD4$^+$ T cells. We analyzed the RNA-seq data (Figure 3H and Supplemental Tables 1 and 2) and ChIP-seq data (Supplemental Table 3), identifying 161 differentially expressed genes (Figure 6A). Among these potential downstream target genes, we identified an obvious peak in the promoter regions of the *Bcl6* and *Il13* genes (Figure 6B). IL-13 was selected as a positive control, which was identified as a target gene of E4BP4 (27, 34). E4BP4 binds to a conserved motif in the *Bcl6* gene promoter (Figure 6B). Enrichment of E4BP4 to *Bcl6* was confirmed by ChIP-qPCR in in vitro–polarized *E4bp4*-cKI Tfh-like cells (Figure 6C).

We previously demonstrated that E4BP4 binds to the promoter region of *CD40LG* and alters histone modifications (35). Based on this, we hypothesized that E4BP4-mediated inhibition of *Bcl6* gene expression might require inhibitory epigenetic modifications. In the *E4bp4*-cKI Tfh-like cells, we found a reduced level of H3 acetylation and an increased level of H3K27 trimethylation in the *Bcl6* gene promoter regions, as compared with the WT control (Figure 6D). Consistently, the Tfh-like cells from *E4bp4*-cKO mice exhibited an increased level of H3 acetylation but a decreased level of H3K27 trimethylation in the *Bcl6* gene promoter region, as compared with their WT littermates (Figure 6E). Enrichment of histone deacetylase HDAC1 and histone methyltransferase EZH2 decreased in Tfh cells from *E4bp4*-cKO mice compared with their WT littermates (Figure 6F). These data suggested that E4BP4 epigenetically regulated *Bcl6* gene transcription in Tfh-like cells. In addition, we observed the similar epigenetic regulatory mechanism in the *E4bp4*-cKO Th1 subsets (in vitro–polarized) (Supplemental Figure 14A), although BCL6 protein expression in Th1 subsets diminished in the *E4bp4*-cKO mice as compared with the WT mice (Supplemental Figure 14B).

We further tested the physical interaction between E4BP4 and EZH2, and between E4BP4 and HDAC1. In line with the above data, we showed that E4BP4 interacted with both HDAC1 and EZH2 (Figure 6, G–I) in the *E4bp4*-cKI Tfh-like cells, whereas no interaction was observed between E4BP4 and another epigenetic modifier, p300 (Supplemental Figure 15, A and B). In summary, these data demonstrated that E4BP4 overexpression repressed *Bcl6* expression by recruiting HDAC1 and EZH2, thus enhancing the level of H3K27 trimethylation and reducing the level of H3 acetylation.

*The role of phosphoserine-defective E4BP4 is impaired in human Tfh cell differentiation*. To investigate the function of E4BP4 in regulating human Tfh cell differentiation, CD4$^+$ T cells from PBMCs of healthy donors were transfected with an E4BP4 overexpression plasmid (Supplemental Figure 16A). CD4$^+$ T cells were then cultured under Tfh polarization conditions. Following transfection with the expression plasmid (E4BP4-over), the percentage of CD4$^+$CXCR5$^+$PD-1$^+$ Tfh cells decreased by 38%, with reduced protein expression of BCL6 and IL-21 as compared with those in the empty vector (EV) group (Figure 7, A and B).

Consistently, cells transfected with E4BP4 small interfering RNAs (siRNAs) (Supplemental Figure 16B) appeared to present a higher proportion of Tfh cells, as well as an elevated expression of BCL6 and IL-21, as compared with the negative control (NC) (Figure 7, C and D).

To further understand the regulation of *BCL6* gene transcription by E4BP4, we tested the luciferase activity of a luciferase reporter gene construct containing human *BCL6* gene promoter with an E4BP4-binding motif. E4BP4 overexpression resulted in a marked decrease in the luciferase activity as compared with the wild-type reporter construct. However, the suppression observed in luciferase activity was rescued when the E4BP4 binding motif was mutated (Figure 7E), indicating that E4BP4 binding might regulate *BCL6* promoter activity.

We then investigated whether E4BP4 is regulated by post-translational modifications that might influence its functions. Phosphorylation of E4BP4 at the Ser301 and Ser353 sites is important for NK cell development (36), but how phosphorylation of E4BP4 influences Tfh cells remains unknown. We then constructed E4BP4 expression plasmids containing the E4BP4 cDNA sequence (WT) or containing mutations at Ser301 and/or Ser353 (SE-Mu301, SE-Mu353 and SE-Mu 301+353) (Figure 7F). GFP expression was detected by flow cytometry to confirm the transfection efficiency (Supplemental Figure 17A). Immunoprecipitation (IP) was performed with an anti–phosphoserine antibody to detect E4BP4 phosphorylation level in human $CD4^+$ T cells expressing mutant version of E4BP4 (Supplemental Figure 17B). The E4BP4 phosphorylation level decreased in the groups transfected with the mutant E4BP4, especially in the SE-Mu301 + 353 group, as compared with the WT control. Total E4BP4 expression was confirmed in each group (Supplemental Figure 17C).

Subsequently, we sought to ascertain whether phosphorylation of E4BP4 would affect its function in regulating Tfh cell differentiation. To this end, human $CD4^+$ T cells were transfected with WT or mutant forms of E4BP4 and then cultured under Tfh cell polarization conditions. We found that the potential of $CD4^+$ T cells to differentiate into Tfh cells was inhibited following transfection with the WT E4BP4 cDNA construct to a greater degree than the empty control; however, the cells transfected with the mutant E4BP4 cDNA constructs were compensated for suppressive capacity of WT E4BP4 (Figure 7, G and H).

Subsequently, we investigated whether expression of the mutant E4BP4 would alter the binding of E4BP4 to *BCL6* promoter. We first confirmed FLAG-E4BP4 expression in the Jurkat cells following transfection with the WT or mutant E4BP4 cDNA constructs (Supplemental Figure 18). ChIP-qPCR was then performed to evaluate epigenetic modifications of the *BCL6* gene in Jurkat cells following expression of WT or mutant E4BP4 cDNA constructs. The binding of E4BP4 to the *BCL6* promoter was abrogated in Jurkat cells that were transfected with the mutant E4BP4 cDNA constructs (Figure 7I, left). The H3 acetylation level was further enriched, whereas the H3K27 trimethylation level showed a decrease in the groups transfected with the mutant E4BP4 cDNA constructs as compared with the WT E4BP4 group (Figure 7I, middle and right). In summary, expression of the mutant E4BP4 reduced the ability of E4BP4 to inhibit Tfh cell differentiation and BCL6 expression.

Additionally, we characterized the impact of the phosphorylation of E4BP4 on T cell activation. The activated naive $CD4^+$ T cells and $CD4^+$ T cells transfected with the WT E4BP4 cDNA construct exhibited decreased percentages of $CD4^+CD40L^+CD69^+$ cells as compared with the cells transfected with EV. However, the ability of E4BP4 to inhibit T cell activation was abolished in cells transfected with mutant E4BP4 cDNA constructs (Supplemental Figure 19, A and B). No radical change was detected in the number of apoptotic cells in each group, implying that transfecting expression vectors had no obvious influence upon cell apoptosis (Supplemental Figure 19C).

*Defective phosphorylation of E4BP4 reduced its suppressive function in SLE*. Patients with SLE exhibit increased frequencies of Tfh cells and high titers of autoantibodies. Our previous studies, together with the result of the Western blots (Supplemental Figure 20A), showed an increased expression of E4BP4 in $CD4^+$ T cells from patients with SLE as compared with healthy controls (35, 37). Herein we measured E4BP4 protein expression in peripheral blood $CD4^+$ T cells from healthy donors and patients with inactive SLE and active SLE by flow cytometry (Figure 8A). Moreover, we determined E4BP4 expression in other types of autoimmune diseases, finding that the E4BP4 expression levels increased in autoantibody-mediated diseases such as rheumatoid arthritis (RA), systemic sclerosis (SSc), pemphigus, and SLE as compared with the healthy controls. Clearly, E4BP4 was most abundant in active SLE (Supplemental Figure 20B). Peripheral E4BP4 expression was significantly correlated with serum anti-dsDNA (Supplemental Figure 20C). In addition, we observed an increased expression of E4BP4 in the SLE PBMC $CD45RA^-CXCR5^{hi}$ Tfh cells compared with that in the $CD45RA^-CXCR5^{lo}$ and $CD45RA^+$ cells (Figure 8B).

To investigate the phosphorylation level of the E4BP4 protein in SLE $CD4^+$ T cells, we detected the phosphorylated E4BP4 protein in patients with SLE and in healthy controls. We observed a significantly reduced phosphorylated E4BP4 relative to total E4BP4 in the SLE $CD4^+$ T cells compared with that of healthy controls (Figure 8C). We concluded that E4BP4-mediated inhibition of Tfh cell differentiation was disrupted in the patients with SLE.

## Discussion

We previously reported the protective role of E4BP4 in SLE involving a reduction of T cell self-reactivity (35), but how E4BP4 regulates T cell–mediated autoimmune responses has not yet been established. In the present study, we documented a role of E4BP4 in regulating Tfh cell differentiation. E4BP4 was prominently upregulated in Tfh cells. The upregulated E4BP4 can directly bind to the promoter region of *Bcl6*, recruiting EZH2 and HDAC to inhibit Bcl6 expression and Tfh cell differentiation. Serine 301 and serine 353 phosphorylation may be important with regard to maintaining the role played by E4BP4 in regulating Tfh cell differentiation. Nonetheless, in patients with SLE, reduced E4BP4 phosphorylation was detected, suggesting that the repressive regulation by E4BP4 might be compromised in SLE.

Although it remains uncertain why E4BP4 increased in the Tfh cells, we can combine previous studies with our data to put forward the following hypotheses. First, E4BP4 expression is enhanced in both exhausted and anergic T cells, and the high

expression of E4BP4 in T cells is well documented (38). Other studies have reported that calcium ions can directly affect the expression of E4BP4, and calcium ions are known to serve as an important indicator for measuring T cell activation. According to our data, the expression of E4BP4 upon stimulation with TCR and IL-12 or TGF-β was not altered compared with its expression in Th0 cells. This is consistent with a previous study that shows that E4BP4 expression is altered by several cytokines in T cells, but not by IL-12 and TGF-β (39). Furthermore, although we did not observe a significant role of IL-12 in upregulating E4BP4 expression, the principal cytokines responsible for Tfh cell differentiation in mice are IL-6 and IL-21 (40). Additionally, our assay was performed in mice cells, though TGF-β is a negative regulator for mice Tfh cell differentiation (41). In combination, IL-12 and TGF-β are indispensable for human Tfh cell differentiation. However, the role they play in regulating mouse Tfh cells is controversial. Moreover, studies of $CD8^+$ T cells have shown that E4BP4 shows a significant increase under the induction of lymphocytic choriomeningitis virus (LCMV); this suggests that E4BP4 is highly sensitive in the immune response of specific viruses (39). Consistently, as we detected E4BP4 expression in KLH- and SRBC-immunized mice, the high expression of E4BP4 in Tfh cells also confirms that E4BP4 is an immune-sensitive gene.

Mice displaying specific deletion of *E4bp4* in $CD4^+$ T cells resulted in a slightly biased T cell compartment. Interestingly, the biased $CD4^+$ and $CD8^+$ T distributions in unimmunized *E4bp4*-cKO mice were normalized following antigen immunization. The transcriptome changes between *E4bp4*-cKO and the WT Tfh-like cells displayed a group of Tfh signature genes, such as *Il21*, *pou2af1*, *Bcl6*, *TCf7*, and *Cd40lg*, which were enriched in the *E4bp4*-cKO group. However, some Tfr signature genes, such as *FoxP3*, *Il10*, and *Ctla4,* were observed to decrease in the *E4bp4*-cKO Tfh-like cells. Upon antigen immunization of *E4bp4*-cKO mice, the proportion of Tfh cells was enhanced, accompanied by an increase in Treg cells, and there was a proportional decrease in Tfr cells. The specific role of E4BP4 in Tfr cells requires further investigation. Even if GC B cell frequency and antigen-specific antibodies increased in the *E4bp4*-cKO mice, no alteration in affinity maturation was observed. This could be a decrease of Tfr cells in follicular T cell pools. The in vitro stimulation assay, which evaluates cell-intrinsic Tfh effector function independently from Tfh differentiation (42), suggested that the *E4bp4*-cKO Tfh-like cells have a comparable stimulatory capacity to that of the WT Tfh-like cells. This phenomenon is not surprising, because the number of Tfh cells sorted from the *E4bp4*-cKO or WT mice was equal, and E4BP4 might be acting mainly as a regulator in Tfh cell differentiation, although it has no effect on promoting IgG production by B cells.

The homeostasis and fate of the immune system require both positive and negative feedback mechanisms in order to adjust, and the negative feedback mechanism plays an important role in preventing the occurrence of autoimmunity (43). The negative feedback mechanism of T cell activation is usually mediated by cosuppressor molecular feedback inhibition (44). The most frequently studied corepressor molecules include CTLA-4, the programmed cell death protein 1 (PD-1), the B and T lymphocyte attenuator (BTLA), the SLAM family, the T cell immunoglobulin mucin 3 (TIM-3), and the TNF receptor superfamily (45). Inhibition of T cell activation by these negative molecules can modulate immune responses and peripheral tolerance and avert inflammation-induced tissue damage, thus preventing multiple autoimmune diseases. An understanding of the mechanism of negative feedback regulation is therefore of great significance in the treatment of autoimmune diseases. In $CD4^+$ T cells, many negative feedback mechanisms exist. For example, IL-6, IL-23, and IL-21 can activate STAT3 to promote the differentiation of Th17 cells. However, activation of STAT3 upregulates the inhibitory protein SOCS3, thus forming a self-limiting autocrine feedback loop to inhibit Th17 cell differentiation (46–48). Notwithstanding, the negative feedback regulation of Tfh cells is not completely understood. One very interesting challenge therefore involves exploring elements that effectively govern Tfh differentiation through feedback inhibition, which is important for accurate control of the immune response.

E4BP4 can directly bind to the promoter region of the *Bcl6* gene, inhibiting its transcription through epigenetic modifications in Tfh-like cells. However, epigenetic regulation of the *Bcl6* gene by E4BP4 is not only restricted in the Tfh cells; the effects of E4BP4 deficiency on Bcl6 expression in the Th1 cells was different from those observed in the Tfh cells. Surprisingly, Bcl6 gene expression presented a slight decrease in the Th1-skewed cells with E4BP4 deficiency, suggesting that Bcl6 is also regulated by other mechanisms. In the Th1 cells, T-bet functionally recruits Bcl-6 to the Ifng locus in Th1 cell differentiation to repress its activity, thus preventing overloads of IFN-γ (49). In turn, a decrease in Bcl6 expression in the Th1 cells could reduce its repressive effect on Ifng, leading to greater expression of IFN-γ. This is consistent with our observation in the *E4bp4*-cKO Th1-skewed cells, although no significant change was detected in IFN-γ production. However, we did observe a slight increase (Supplemental Figure 6A) in relation to the WT cells. This might account for the decrease in Bcl6 expression and the altered epigenetic regulation of Bcl6 in the Th1 cells.

E4BP4 has been demonstrated to constitute a survival factor for many cells and, in the case of immune cells, it is necessary for controlling autoimmune conditions. E4BP4 was shown to control autoimmune responses in the experimental autoimmune encephalomyelitis (EAE) model. Results were supported by a noteworthy development of EAE in E4BP4 knockout mice (27). In many cases, E4BP4 is frequently shown to play a part in regulating cytokine generation, which implies that the antiinflammatory role of E4BP4 in immune responses was achieved by regulating cytokine production. Antiinflammatory cytokines such as IL-10 can be induced by E4BP4 in multiple T cell subsets (27, 28). E4BP4-deficient effector T cells generated less IL-10 and showed serious defects in the control of immune responses, thus resulting in accelerated central nervous system autoimmunity and colitis (27, 29, 50). Moreover, E4BP4 restricts macrophage-mediated inflammation by controlling IL-12 p40 production, thereby negatively regulating innate immunity (51). Interestingly, in the absence of E4BP4, production of IL-5, IL-9, and IL-13 increases (27, 28). These cytokines are associated with B cell activation, but the possible roles of IL-5 and IL-13 in the pathogenesis of lupus have not been extensively evaluated. Moreover, E4BP4-knockout Th17 cells exhibit increased

IL-17 expression and greater susceptibility to inflammatory diseases (29). E4BP4 suppresses intestinal Th17 differentiation and reduces IL-17A production (29), and IL-17A is known to be associated with inflammatory responses in subjects with SLE, clearly giving rise to inflammation and damage of target organs in SLE models (52, 53).

In our study we found that E4BP4 is upregulated in several autoimmune diseases, including SLE, RA, or SSc (Supplemental Figure 20B). Two factors may be contributing to increased E4BP4 expression in active SLE as compared with inactive SLE and controls. First, E4BP4 is associated with transcription repression in inhibiting Th17 cells (29), as well as Tfh cell differentiation and humoral responses. This might generate a feedback mechanism of E4BP4 expression in autoimmune conditions intended to limit the inflammatory responses, even though the high expression of unphosphorylated E4BP4 is less functional in SLE according to our data. The expression of E4BP4 expression in Tfh1/Tfh2/Tfh17 populations has not been addressed in the present research, but it is of great importance with regard to understanding the function of E4BP4 in different Tfh cell subtypes. Second, it has been reported that E4BP4 is markedly induced by glucocorticoid (dexamethasone) (54). In our case, many patients, especially those with active SLE (more severe), were treated with high doses of glucocorticoid, and this could be another factor accounting for the high E4BP4 expression.

The phosphorylation-defective E4BP4 presented impaired biological activity in regulating human T cell activation and Tfh cell differentiation and, importantly, the mutants had an antagonistic effect on the WT E4BP4 protein, leading to increased Tfh cell differentiation. A previous study has shown phosphorylation to be important for the DNA binding activity of E4BP4 (55). On comparing the activity of WT E4BP4 with mutant forms lacking serine phosphorylation, greater percentages of Tfh cells were induced in naive $CD4^+$ T cells following transfection with mutant plasmids compared with the WT group. This implies that deficient serine phosphorylation levels directly lead to a loss of the inhibitory activity of E4BP4 during Tfh cell differentiation. These findings indicated that phosphorylation is indispensable in order for E4BP4 to regulate Tfh cell differentiation, as removing the phosphorylation sites reduces E4BP4 activity and ultimately promotes Tfh cell differentiation. However, our finding is inconsistent with a recent report that indicated that the transcriptional activity of E4BP4 was negatively correlated with the phosphorylation level in NK cells (36). We speculate that this discordance may be due to the different regulatory mechanisms of E4BP4 in different cell types. In addition, both PD98059 and U0126, 2 selective inhibitors for MEK1/2, completely suppress IL-3–induced E4BP4 phosphorylation in Ba/F3 cells (56). In our study, the PD98059 and U0126 treatments substantially reduced E4BP4 phosphorylation in the induced $CD4^+$ T cells cultured under Tfh polarized conditions (data not shown).This appears to show that E4BP4 phosphorylation in $CD4^+$ T cells was dependent on the MAPK signaling pathway. Abnormalities in the MAPK signaling pathway have been reported in SLE T cells and include an impaired extracellular signal-regulated kinase (ERK) signaling cascade (57), which may explain the increased E4BP4 expression with deficient phosphorylation in lupus $CD4^+$ T cells.

In conclusion, our study revealed that E4BP4 constitutes a new regulator for controlling Tfh cell differentiation. E4BP4 expression was elevated in Tfh cells but inhibits Tfh cell differentiation in a negative feedback manner. Our findings demonstrate that E4BP4 has an unrecognized capacity for directly combining epigenetic and transcriptional regulatory mechanisms in order to regulate the Tfh lineage; thus, modulation of its phosphorylation level could potentially inhibit Tfh cell–mediated humoral immune responses in SLE.

## Methods

*Mice*. C57BL/6 mice were obtained from the Slack Company. *Rag2*$^{-/-}$ mice were obtained from the Shanghai Research Center for Model Organisms. *E4bp4*-cKO mice and *E4bp4*-KO mice were provided by Masato Kubo (RIKEN Institute, Tokyo, Japan) (27). For the generation of the E4BP4-transgenic mice, *E4bp4*-Rosa26 knockin mice were provided by the Shanghai Biomodel Organism Science and Technology Development Co. Ltd. We generated the *E4bp4*-cKI mice by crossing *E4bp4*-Rosa26 knockin mice with mice expressing Cre recombinase from the T cell–specific *Cd4* promoter (Cd4-Cre). We confirmed the genotypes of the mice by performing PCR analyses of genomic DNA isolated from mouse tails and using the following primers: *E4bp4*-KO mice: forward 5′-GATTGCATGGGTCCAAGTCT-3′, reverse 5′-CACAAGGACACCCAGACAGA-3′; *E4bp4*-cKO mice: forward 5′-TCAAAGTGGAGGCTTTGGAC-′3, reverse 5′-CACAAGGACACCCAGACAGA-3′; *E4bp4*-cKI mice primer 1: forward 5′-AAAGTCGCTCTGAGTTGTTAT-3′, reverse 5′-GGAGCGGGAGAAATGGATATG-3′; *E4bp4*-cKI mice primer 2: forward 5′-GGACAGCGAGTTTGAAGGCATGC-3′, reverse 5′-GGAGCGGGAGAAATGGATATG-3′. Mice aged 6 to 12 weeks were used in all experiments.

*Study subjects*. For the present study, 60 patients with SLE who met the requirements of the Revised Criteria of the American College of Rheumatology (58) for SLE and age-matched healthy females were recruited from outpatient dermatology clinics and inpatient wards. Exclusion criteria were previously described (59). Activity categories were defined on the basis of Systemic Lupus Erythematosus Disease Activity Index (SLEDAI) scores: no activity (SLEDAI = 0–4), mild activity (SLEDAI = 5 to 10), moderate activity (SLEDAI = 11 to 14), and high activity (SLEDAI ≥ 15). Human tonsil tissues were obtained from a routine tonsillectomy at The Second Xiangya Hospital, Central South University. Mononuclear cells were isolated from human tonsils and labeled as previously described (60). Data were acquired with a flow cytometer and analyzed with the use of FlowJo software (Tree Star). Patient information is shown in Supplemental Table 4.

*KLH and SRBC immunization*. Mice were immunized with s.c. administered KLH (0.5 mg/mL) (MilliporeSigma) emulsified in CFA, and $2 \times 10^9$ SRBCs (Beijing Berseebio Company). Splenic and lymph node cells were stained with fluorochrome-labeled antibodies and analyzed with FlowJo software. For the memory responses, lymphocytes were restimulated and cultured with different doses of KLH for 3 days. Subsequently, the supernatant of the cell culture was collected for IL-21 and Bcl6 detection by ELISA and RT-PCR. Reagents are listed in Supplemental Table 5.

*Pristane-induced lupus mouse model*. For lupus-like disease induction, the *E4bp4*-cKO and the WT mice were administered one i.p. injection of 500 μL saline (as a control) or pristane (MilliporeSigma). For the ex vivo analysis, experimental mice were sacrificed 8 months after the pristane injection as previously described (59).

*In vitro differentiation of mouse T cells*. The protocol for in vitro–polarized Th1, Th2, Th17, and Treg cells in mice was previously described (61). For polarized Tfh cells, 4 μg/mL anti-CD3 antibody (BD Biosciences, catalog 553057; 4 μg/mL) in PBS was incubated in 24-well round-bottom tissue culture plates at 4°C overnight. Naive $CD4^+$ T cells were then activated with anti-CD28 (BD Biosciences, catalog 553294; 1 μg/mL), anti–IFN-γ (BD Biosciences, catalog 554430; 10 μg/mL), and anti–IL-4 antibodies (BD Biosciences, catalog 554385; 10 μg/mL), and anti–TGF-β (Thermo Fisher Scientific, catalog 16-9243-85; 20 μg/mL) plus cytokines IL-6 (PeproTech; 10 ng/mL) and IL-21 (PeproTech; 10 ng/mL). Cells were incubated at 37°C under 5% $CO_2$ conditions for 3 to 5 days. The percentages of in vitro–polarized Th1, Th2, Th17, Treg, and Tfh cells were analyzed by flow cytometry.

*In vitro human Tfh cell differentiation*. Naive $CD4^+$ T cells were purified from PBMCs with the human Naive $CD4^+$ T Cell Isolation Kit (Miltenyi).Purity ($CD4^+CD45RA^+$) was over 95%. Anti-CD3 antibodies (Calbiochem, catalog 217570; 4 μg/mL) were precoated in a 24-well plate at 4°C overnight, and naive $CD4^+$ T cells were plated into the medium with anti-CD28 antibodies (Calbiochem, catalog 217669; 1 μg/mL) and cultured with recombinant human IL-21 (PeproTech; 20 ng/mL), recombinant human IL-12 (PeproTech; 5 ng/mL), recombinant human TGF-β (PeproTech; 1 ng/mL), and recombinant human IL-6 (PeproTech; 20 ng/mL) in RPMI 1640 medium (Gibco) supplemented with 10% FBS (HyClone) at 37°C in a 5% $CO_2$ atmosphere for 3 to 5 days, or collected immediately for subsequent experiments.

*Flow cytometry*. Single-cell suspensions were fluorescently labeled as previously described (59). In the case of FoxP3, BCL6, and E4BP4 staining, a FoxP3 staining kit (BD Biosciences) was used for intracellular staining. Stained cells were analyzed by means of BD FACSCalibur and FACSAria II flow cytometers and FlowJo software (Tree Star).

The following antibodies were used: FITC anti–human CD4 (BD Biosciences, catalog 550628), APC mouse anti–human CD69 (BD Biosciences, catalog 555533), PE mouse anti–human CD154 (BD Biosciences, catalog 555700), PE anti–human IL-17A (BD Biosciences, catalog 560487), Alexa Fluor 647 anti–human IFN-γ (BioLegend, catalog 502516), PE anti–human IL-4 (BioLegend, catalog 500704), APC-Cy7 anti–human Bcl-6 (BD Biosciences, catalog 563581), PE-CY7 anti–human CD185 (BioLegend, catalog 356923), Alexa Fluor 647 anti–human FOXP3 (BD Biosciences, catalog 561184), PE anti–human CD278 (Thermo Fisher Scientific, catalog 12-9185), APC anti–human CD279 (Thermo Fisher Scientific, catalog 85-17-2799-42), human E4BP4 (NFIL3) monoclonal antibody (Thermo Fisher Scientific, catalog 12-9812-42), FITC anti–mouse CD4 (BioLegend, catalog 100406), PerCP-Cy5.5 rat anti–mouse Foxp3 (BD Biosciences, catalog 563902), APC-Cy7 mouse anti–Bcl-6 (BD Biosciences, catalog 563581), Biotin rat anti–mouse CXCR5, APC-Cy7 rat anti–mouse CD62L (BD Biosciences, catalog 560514), PE-Cy7 rat anti–mouse CD44 (BD Biosciences, catalog 560569), APC hamster anti–mouse CD279 (PD-1) (BD Biosciences, catalog 562671), PE rat anti–mouse CD278 (ICOS) (BD Biosciences, catalog 552146), PE hamster anti–mouse CD95 (BD Biosciences, catalog 554258), Alexa Fluor 647 anti–mouse T and B cell activation antigen (BD Biosciences, catalog 561529), FITC anti–mouse CD45R/B220 (BD Biosciences, catalog 553087), and mouse E4BP4 (NFIL3) monoclonal antibody (BD Biosciences, catalog 551960; Thermo Fisher Scientific, catalog 12-5927-82).

*Immunofluorescence*. For confocal microscopy, naive $CD4^+$ T cells, anti-CD3/CD28–activated naive $CD4^+$ T cells, and in vitro–polarized Tfh cells were fixed and permeabilized with a FoxP3 staining kit. Images were captured with an LSM 510 confocal microscopy system (Leica). For tissue samples, mLNs were fixed with formalin and embedded with paraffin. The following antibodies were used: E4BP4 antibody (Santa Cruz, sc-74415), anti-mouse Alexa Fluor 594 (Thermo Fisher Scientific, catalog A-21201), anti-peanut agglutinin (PNA) (Vector Laboratories, catalog BA-0074), and anti-CD3 antibody (Abcam, catalog ab5690). Images were obtained with the use of a laser scanning microscope (Olympus).

*Transfection of the E4BP4 overexpression plasmid or siRNA*. An E4BP4-pCDNA3.1 overexpression plasmid and siRNA were described in a previous study (35). For phospho-mutant plasmid transfections, the Ser301 mutant (SE-Mu301), Ser305 mutant (SE-Mu305), and Ser301 and Ser305 double mutant (SE-Mu301 + 353) were generated in the E4BP4 cDNA (S301A and S353A) in the pCDNA3.1 plasmid expression vector with an additional FLAG tag, which was purchased from RiboBio Co., China. Purified naive $CD4^+$ T cells or $CD4^+$ T cells were transfected with a Human T cell Nucleofector Kit and an Amaxa nucleofector (Lonza). $CD4^+$ T cells were then resuspended in human T cell nucleofector solution, and E4BP4-siRNA (HSS109204, Thermo Fisher Scientific) was added. E4BP4 siRNA and Entransfer-R (18668-06, Engreen) reagents were prepared by mixing them with OptiMEM. Following incubation at room temperature for 5 minutes, the siRNAs and transfection reagents were mixed and incubated at room temperature for 30 minutes. The transfection cocktail was added to each well and cells were incubated at 37°C. The complete medium was replaced after 6 hours.

*Coculture of Tfh and B cell subsets*. The $CD4^+CD44^+CD62L^-CXCR5^+PD\text{-}1^+$ Tfh cells and the $B220^+GL\text{-}7^+FAS^+$ GC B cells were sorted and plated in U-bottom 96-well plates at a density of $1 \times 10^4$ Tfh cells/well, and the B cells were added at a ratio of 1:1 (Tfh/B) for 7 days. We performed the cultures in RPMI supplemented with penicillin (50 U/mL), streptomycin (50 μg/mL), and 10% FBS, plus NP-KLH (MilliporeSigma), anti-CD3/CD28 (BD Biosciences, catalog 553057 and 553294), CD40 monoclonal antibody (Thermo Fisher Scientific, catalog 16-0402-82), AffiniPure $F(ab')_2$ fragment goat anti–mouse IgM, μ chain–specific (Jackson Immunoresearch; catalog 115-006-020), murine IL-4, and IL-2 (PeproTech).

*Quantitative RT-PCR*. Total RNA was extracted from cells infiltrated in TRIzol reagent (Thermo Fisher Scientific). Additionally, cDNA was generated by means of reverse transcription with a PrimeScript RT reagent kit, following the manufacturer's instructions. The transcript was analyzed for the expression of several genes with a LightCycler 96 System (Roche). Primer sequences are listed in Supplemental Table 6.

*ELISA*. Antibody titers of anti-KLH–specific or SRBC-specific IgGs and IgM in serum were measured with ELISA. For KLH-specific antibody detection, wells were coated with 10 mg/mL KLH overnight at 4°C. For anti-SRBC antibody analysis, wells were coated with SRBC membrane protein overnight at 4°C. Wells were blocked with 10% FCS and diluted serum was incubated in the wells for 1 hour at room temperature. A peroxidase-labeled Fc-specific anti–mouse IgG or IgM detection Ab was used. Serum levels of the anti-snRNP (Alpha Diagnostic; catalog 5410) and anti–dsDNA autoantibodies (Alpha Diagnostic; catalog 5120) were measured with the use of ELISA kits

as previously described (59). For affinity maturation, high-affinity and total hapten 4-hydroxy-3-nitrophenyl acetyl–specific (NP-specific) antibodies were measured by ELISA with 10 mg/mL NP–2-BSA or NP–27-BSA (Bioresearch Technologies) as the coating reagent, respectively. Diluted serum was incubated in the wells for 1 hour at room temperature. NP-specific IgG1 was detected with the use of goat polyclonal anti–IgG1 HRP (SouthernBiotech; catalog 1071-05) and developed with tetramethylbenzidine.

*Evaluation of renal histopathological features and immunofluorescence staining*. We stained paraffin-embedded sections of renal tissues with H&E. Histopathological features of glomerular lesions were semiquantitatively scored for severity in a double-blinded manner. The histological signs of lupus nephritis were assessed by pathologists. Frozen sections of mouse kidneys were fixed with cold acetone and stained for mouse C3 by indirect immunofluorescence with a rat anti–C3 antibody (Abcam; catalog 11H9) and Cy3-conjugated goat anti–rat IgG (Servicebio, catalog GB21302). The same procedure was performed for mouse IgG by direct immunofluorescence with Alexa Fluor 488–conjugated goat anti–mouse IgG (Abcam; catalog 150113), respectively.

*Coimmunoprecipitation*. Anti-Flag antibody (Cell Signaling Technology, catalog 14793) was used to immunoprecipitate E4BP4 before Western blotting of anti-EZH2 (Abcam, catalog ab186006) and anti-HDAC1 (Active Motif, catalog 40967). Immunoblotting was performed according to the ECL procedure. Cells were directly lysed in Laemmli sample buffer and separated on a 10% SDS-PAGE gel. Proteins were blotted onto a PVDF membrane (Bio-Rad Laboratories) and blocked with 5% low-fat milk and 1% Tween-20 in PBS. Membranes were incubated with the aforementioned antibodies and washed 3 times with PBST (PBS containing 1% Tween-20). For detection of E4BP4 phosphorylation, anti–phosphoserine antibody (Cell Signaling Technology, catalog 9631) was used to immunoprecipitate phosphorylated E4BP4. Anti-E4BP4 antibody (Cell Signaling Technology, catalog 14312S) was employed for immunoblotting.

*Western blotting*. Cells were lysed in radioimmunoprecipitation assay (RIPA) buffer (MilliporeSigma) and equal amounts of total proteins were separated by SDS-PAGE with 8% polyacrylamide gels (Invitrogen), and then transferred to PVDF membranes (Millipore), followed by antibody staining and detection of anti-E4BP4 (1:1000) (Cell Signaling Technology, catalog 14312S), anti-HDAC1 (1:1000) (Active Motif, catalog 40967), anti-EZH2 (1:500) (Abcam, catalog ab186006), anti-FLAG (1:1000) (Cell Signaling Technology, catalog 14793), and anti–β-actin (1:1000) (Abcam, catalog ab6276).

*Chromatin immunoprecipitation PCR*. *E4bp4*-cKI and *E4bp4*-cKO splenocyte CD4$^+$ T cells and Jurkat cells (purchased from ATCC) transfected with the E4BP4 overexpression plasmid or phospho-mutant plasmids were isolated. We used chromatin immunoprecipitation (ChIP) with anti-FLAG (Cell Signaling Technology, catalog 14793), anti-E4BP4 (Cell Signaling Technology, catalog 14312S), anti–acetyl-histone H3 (Active motif; catalog 39139), anti-H3K27me3 (Active Motif; catalog 39155), anti-EZH2 (Abcam, catalog ab186006), and anti-HDAC1 antibodies (Active Motif, catalog 40967) to detect *Bcl6* enrichment with a ChIP kit (Millipore). The detailed protocols were previously described (59). Immunoprecipitated DNA and input DNA were assessed by means of real-time PCR. The resulting DNA fragments were purified and subjected to PCR with the use of primers encompassing the D-box region of the mouse Bcl6 gene promoter. The primers used in the present study were: forward (m*Bcl6*-F: 5′-ATGAACCCACCGAAAACTGC-3′) and reverse (m*Bcl6*-R: 5′-GACGAGGGAGGGAGAAAACA-3′) for the mouse promoter region; forward (*BCL6*-F: 5′-aaaatcccaagccaccacac-3′) and reverse (*BCL6*-R: 5′-aagcagttttcggtgggttc-3′) for the human promoter region.

*Dual-luciferase reporter assay*. For luciferase reporter assays, the upstream regions of the *BCL6* containing WT or mutated E4BP4 binding sites were subcloned into the pGL3-basic vector (Promega). HEK293T cells were cultured in RPMI 1640 supplemented with 10% FBS. Cells were plated in a 24-well plate at a density of $1 \times 10^6$ cells/well. Following overnight incubation, cells were cotransfected with 10 ng firefly luciferase reporter vector containing the WT or Mu-Bcl6 sequence, 10 ng of the pEGFP-C1 E4BP4 plasmid, or the negative control (pEGFP-C1) by electroporation with Lipofectamine 2000 (Invitrogen) according to the manufacturer's instructions. One day after transfection, luciferase activity was measured by means of the Dual-Luciferase Reporter Assay System (Promega) with a GloMax 20/20 luminometer (Promega).

*Adoptive transfer of T cells and B cells into Rag2$^{-/-}$ mice*. Naive CD4$^+$ T cells were isolated from the WT mice or the *E4bp4*-KO mice with the mouse Naive CD4$^+$ T Cell Isolation Kit (Miltenyi), and B cells were then obtained from the WT mice with a mouse B cell isolation kit. The purity of the naive CD4$^+$ T cells and/or the B cells was detected by flow cytometry and the percentage of positive cells was over 98%. Herein we employed 2 groups of *Rag2*$^{-/-}$ mice; one group was transferred with naive CD4$^+$ T cells and the B cells from the WT mice, and the other group was transferred with naive CD4$^+$ T cells from the *E4bp4*-KO mice and with the B cells from the WT mice. Following 7 days of injection, these 2 groups of mice were immunized with KLH and CFA.

*RNA-sequencing and bioinformatics analysis*. For isolation of the Tfh cells, we collected and cultured total splenocyte naive CD4$^+$T cells from WT and *E4bp4*-cKO mice for 3 days under Tfh conditions. Total RNA samples were extracted by means of TRIzol reagent according to the manufacturer's protocol (Life Technologies) and submitted to Novogene for RNA sequencing, including total RNA sample detection, mRNA enrichment, synthesis of double-stranded cDNAs, end repair/dA-tailing module, fragment selection, and PCR amplification, library detection, and Illumina sequencing. All sequencing data and experimental protocols were submitted to the National Center for Biotechnology Information (NCBI) Gene Expression Omnibus (GEO) in accordance with the MIAME standard (GSE 121389). The method for screening differentially expressed genes between 2 groups was filtered by $P$ value of less than 0.05, and fold-change values were more than 1.2-fold.

*ChIP-Seq and data processing*. Splenocytes and lymphocytes were obtained from the *E4bp4*-cKI mice and the CD4$^+$ T cells were purified with an isolation kit (MiltenyiBiotec) and subjected to ChIP analysis with anti-FLAG. DNA fragments from the ChIP were processed, end-repaired, and ligated to indexed Illumina adaptors followed by PCR. The resulting libraries were sequenced with the Illumina HiSeq-2000 platform. The sequencing quality of ChIP-Seq libraries was assessed by FastQC. The sequenced reads were obtained and mapped to the mouse genome (mm10 assembly) with the use of IGV. Peaks were called with MACS2 version 2.1.0 (model-based analysis of ChIP-Seq). The $Q$ value threshold of enrichment of 0.05 was employed for all data sets. Raw and processed sequencing data are available at the NCBI Gene Expression Omnibus (GEO) under accession number GSE121389.

*Gene set enrichment analysis*. Expression profiling files from Tfh cells versus non–Tfh cells were downloaded from the GEO data set

(GSE16697) and compared with our RNA-Seq data of E4BP4-bound peaks (GSE121389) by means of GSEA, performed with GSEA v2.0.13 software. We implemented the GSEA according to a paper previously published by Xu et al. (62).

*Statistics*. Statistical analyses were conducted with Prism 6.0 software (GraphPad). We employed an unpaired 2-tailed *t* test with a 95% confidence interval to calculate *P* values. Data are mean ± SD. Comparisons among multiple groups were performed with 1-way ANOVA. Pearson's correlation coefficients were calculated to determine the strength of the correlations between 2 variables. *P* values of less than 0.05 were considered to be significant. Sequence data supporting the findings of this study have been deposited in the Gene Expression Omnibus with primary accession code GSE121389.

*Study approval*. All animal procedures were approved by the Animal Care and Use Committee of the Laboratory Animal Research Center at the Second Xiangya Medical School, Central South University. All human studies were approved by the Ethics Committee of the Second Xiangya Hospital, Central South University, China, and all patients, including those with SLE, RA, pSS, psoriasis, and pemphigus, provided written informed consent.

## Author contributions

ZW and MZ conceptualized the studies and wrote the manuscript. ZW and JY analyzed the data and interpreted the results. ZW, JY, LL, LH, YH, JO, AL, and XM conducted the experiments with the help from SR and WZ. HW and AY provided suggestions for the study. QL conceptualized, supervised, and revised the manuscript. ZW and MZ share first authorship, and the order in which they are listed was determined by workload.

## Acknowledgments

The present research was supported by the National Natural Science Foundation of China (projects 81522038, 81430074, 81830097, 81874243, and 81903221), the innovation project of the Chinese academy of medical sciences (Research Unit 2019-I2M-5-033), the Key project for international and regional cooperation in science and technology innovation of Hunan province (2019WK2081), the Project for leading talents in science and technology in Hunan province (2019RS3003), and the Fundamental Research Funds for the Central Universities of Central South University (2018zzts262). The present research was also supported by JSPS KAKENHI (S) JP17H06175, Challenging Research (P) JP18H05376, and AMED-CREST JP19gm1110009 grants to Akihiko Yoshimura.

Address correspondence to: Qianjin Lu, Department of Dermatology, The Second Xiangya Hospital, Central South University, 139 Renmin Middle Road, Changsha, Hunan 410011, China. Phone: 86.731.85295860; Email: qianlu5860@csu.edu.cn.

1. Crotty S. Follicular helper CD4 T cells (TFH). *Annu Rev Immunol*. 2011;29:621–663.
2. Tangye SG, Ma CS, Brink R, Deenick EK. The good, the bad and the ugly - TFH cells in human health and disease. *Nat Rev Immunol*. 2013;13(6):412–426.
3. Shekhar S, Yang X. The darker side of follicular helper T cells: from autoimmunity to immunodeficiency. *Cell Mol Immunol*. 2012;9(5):380–385.
4. Kim SJ, et al. Increased cathepsin S in Prdm1$^{-/-}$ dendritic cells alters the $T_{FH}$ cell repertoire and contributes to lupus. *Nat Immunol*. 2017;18(9):1016–1024.
5. Niu Q, et al. Enhanced IL-6/phosphorylated STAT3 signaling is related to the imbalance of circulating T follicular helper/T follicular regulatory cells in patients with rheumatoid arthritis. *Arthritis Res Ther*. 2018;20(1):200.
6. Jacquemin C, et al. OX40 ligand contributes to human lupus pathogenesis by promoting T follicular helper response. *Immunity*. 2015;42(6):1159–1170.
7. Xu H, et al. Increased frequency of circulating follicular helper T cells in lupus patients is associated with autoantibody production in a CD40L-dependent manner. *Cell Immunol*. 2015;295(1):46–51.
8. Huang X, et al. The expression of Bcl-6 in circulating follicular helper-like T cells positively correlates with the disease activity in systemic lupus erythematosus. *Clin Immunol*. 2016;173:161–170.
9. Linterman MA, et al. Foxp3+ follicular regulatory T cells control the germinal center response. *Nat Med*. 2011;17(8):975–982.
10. Alexander CM, Tygrett LT, Boyden AW, Wolniak KL, Legge KL, Waldschmidt TJ. T regulatory cells participate in the control of germinal centre reactions. *Immunology*. 2011;133(4):452–468.
11. Wollenberg I, et al. Regulation of the germinal center reaction by Foxp3+ follicular regulatory T cells. *J Immunol*. 2011;187(9):4553–4560.
12. Sage PT, Sharpe AH. T follicular regulatory cells. *Immunol Rev*. 2016;271(1):246–259.
13. Sage PT, Francisco LM, Carman CV, Sharpe AH. The receptor PD-1 controls follicular regulatory T cells in the lymph nodes and blood. *Nat Immunol*. 2013;14(2):152–161.
14. Chung Y, et al. Follicular regulatory T cells expressing Foxp3 and Bcl-6 suppress germinal center reactions. *Nat Med*. 2011;17(8):983–988.
15. Clement RL, et al. Follicular regulatory T cells control humoral and allergic immunity by restraining early B cell responses. *Nat Immunol*. 2019;20(10):1360–1371.
16. Xu B, et al. The ratio of circulating follicular T helper cell to follicular T regulatory cell is correlated with disease activity in systemic lupus erythematosus. *Clin Immunol*. 2017;183:46–53.
17. Fonseca VR, et al. The ratio of blood T follicular regulatory cells to T follicular helper cells marks ectopic lymphoid structure formation while activated follicular helper T cells indicate disease activity in primary Sjögren's syndrome. *Arthritis Rheumatol*. 2018;70(5): 774–784.
18. Crotty S. T follicular helper cell differentiation, function, and roles in disease. *Immunity*. 2014;41(4):529–542.
19. Liu X, Nurieva RI, Dong C. Transcriptional regulation of follicular T-helper (Tfh) cells. *Immunol Rev*. 2013;252(1):139–145.
20. Baumjohann D, Heissmeyer V. Posttranscriptional gene regulation of T follicular helper cells by RNA-binding proteins and microRNAs. *Front Immunol*. 2018;9:1794.
21. Díaz-Muñoz MD, Turner M. Uncovering the role of RNA-binding proteins in gene expression in the immune system. *Front Immunol*. 2018;9:1094.
22. Yu D, et al. The transcriptional repressor Bcl-6 directs T follicular helper cell lineage commitment. *Immunity*. 2009;31(3):457–468.
23. Cowell IG, Hurst HC. Transcriptional repression by the human bZIP factor E4BP4: definition of a minimal repression domain. *Nucleic Acids Res*. 1994;22(1):59–65.
24. Kashiwada M, et al. IL-4-induced transcription factor NFIL3/E4BP4 controls IgE class switching. *Proc Natl Acad Sci U S A*. 2010;107(2):821–826.
25. Kamizono S, et al. Nfil3/E4bp4 is required for the development and maturation of NK cells in vivo. *J Exp Med*. 2009;206(13):2977–2986.
26. Gascoyne DM, et al. The basic leucine zipper transcription factor E4BP4 is essential for natural killer cell development. *Nat Immunol*. 2009;10(10):1118–1124.
27. Motomura Y, et al. The transcription factor E4BP4 regulates the production of IL-10 and IL-13 in CD4+ T cells. *Nat Immunol*. 2011;12(5):450–459.
28. Kashiwada M, Cassel SL, Colgan JD, Rothman PB. NFIL3/E4BP4 controls type 2 T helper cell cytokine expression. *EMBO J*. 2011;30(10):2071–2082.
29. Yu X, et al. TH17 cell differentiation is regulated by the circadian clock. *Science*. 2013;342(6159):727–730.
30. Kim HS, Sohn H, Jang SW, Lee GR. The transcription factor NFIL3 controls regulatory T-cell function and stability. *Exp Mol Med*. 2019;51(7):80.
31. Lu KT, et al. Functional and epigenetic studies reveal multistep differentiation and plasticity of in vitro-generated and in vivo-derived follicular T helper cells. *Immunity*. 2011;35(4):622–632.

32. Bossaller L, et al. TLR9 deficiency leads to accelerated renal disease and myeloid lineage abnormalities in pristane-induced murine lupus. *J Immunol*. 2016;197(4):1044–1053.
33. Reeves WH, Lee PY, Weinstein JS, Satoh M, Lu L. Induction of autoimmunity by pristane and other naturally occurring hydrocarbons. *Trends Immunol*. 2009;30(9):455–464.
34. Yuan L, et al. HDAC11 regulates interleukin-13 expression in CD4+ T cells in the heart. *J Mol Cell Cardiol*. 2018;122:1–10.
35. Zhao M, et al. E4BP4 overexpression: a protective mechanism in CD4+ T cells from SLE patients. *J Autoimmun*. 2013;41:152–160.
36. Kostrzewski T, et al. Multiple levels of control determine how E4bp4/Nfil3 regulates NK cell development. *J Immunol*. 2018;200(4):1370–1381.
37. Zhao M, et al. Epigenetics and SLE: RFX1 down-regulation causes CD11a and CD70 overexpression by altering epigenetic modifications in lupus CD4+ T cells. *J Autoimmun*. 2010;35(1):58–69.
38. Joseph N, Reicher B, Barda-Saad M. The calcium feedback loop and T cell activation: how cytoskeleton networks control intracellular calcium flux. *Biochim Biophys Acta*. 2014;1838(2):557–568.
39. Zhu C, et al. An IL-27/NFIL3 signalling axis drives Tim-3 and IL-10 expression and T-cell dysfunction. *Nat Commun*. 2015;6:6072.
40. Nurieva RI, et al. Generation of T follicular helper cells is mediated by interleukin-21 but independent of T helper 1, 2, or 17 cell lineages. *Immunity*. 2008;29(1):138–149.
41. McCarron MJ, Marie JC. TGF-β prevents T follicular helper cell accumulation and B cell autoreactivity. *J Clin Invest*. 2014;124(10):4375–4386.
42. Sage PT, Alvarez D, Godec J, von Andrian UH, Sharpe AH. Circulating T follicular regulatory and helper cells have memory-like properties. *J Clin Invest*. 2014;124(12):5191–5204.
43. Nakken B, Alex P, Munthe L, Szekanecz Z, Szodoray P. Immune-regulatory mechanisms in systemic autoimmune and rheumatic diseases. *Clin Dev Immunol*. 2012;2012:957151.
44. Yu D, Vinuesa CG. Multiple checkpoints keep follicular helper T cells under control to prevent autoimmunity. *Cell Mol Immunol*. 2010;7(3):198–203.
45. Pentcheva-Hoang T, Corse E, Allison JP. Negative regulators of T-cell activation: potential targets for therapeutic intervention in cancer, autoimmune disease, and persistent infections. *Immunol Rev*. 2009;229(1):67–87.
46. Maddur MS, Miossec P, Kaveri SV, Bayry J. Th17 cells: biology, pathogenesis of autoimmune and inflammatory diseases, and therapeutic strategies. *Am J Pathol*. 2012;181(1):8–18.
47. Kleinsteuber K, et al. SOCS3 promotes interleukin-17 expression of human T cells. *Blood*. 2012;120(22):4374–4382.
48. Qin H, et al. TGF-beta promotes Th17 cell development through inhibition of SOCS3. *J Immunol*. 2009;183(1):97–105.
49. Oestreich KJ, Huang AC, Weinmann AS. The lineage-defining factors T-bet and Bcl-6 collaborate to regulate Th1 gene expression patterns. *J Exp Med*. 2011;208(5):1001–1013.
50. Farez MF, et al. Melatonin contributes to the seasonality of multiple sclerosis relapses. *Cell*. 2015;162(6):1338–1352.
51. Kobayashi T, et al. NFIL3 is a regulator of IL-12 p40 in macrophages and mucosal immunity. *J Immunol*. 2011;186(8):4649–4655.
52. Martin JC, Baeten DL, Josien R. Emerging role of IL-17 and Th17 cells in systemic lupus erythematosus. *Clin Immunol*. 2014;154(1):1–12.
53. Garrett-Sinha LA, John S, Gaffen SL. IL-17 and the Th17 lineage in systemic lupus erythematosus. *Curr Opin Rheumatol*. 2008;20(5):519–525.
54. Wallace AD, Wheeler TT, Young DA. Inducibility of E4BP4 suggests a novel mechanism of negative gene regulation by glucocorticoids. *Biochem Biophys Res Commun*. 1997;232(2):403–406.
55. Chen WJ, et al. Characterization of human E4BP4, a phosphorylated bZIP factor. *Biochim Biophys Acta*. 1995;1264(3):388–396.
56. Yu YL, et al. MAPK-mediated phosphorylation of GATA-1 promotes Bcl-XL expression and cell survival. *J Biol Chem*. 2005;280(33):29533–29542.
57. Deng C, et al. Decreased Ras-mitogen-activated protein kinase signaling may cause DNA hypomethylation in T lymphocytes from lupus patients. *Arthritis Rheum*. 2001;44(2):397–407.
58. Hochberg MC. Updating the American College of Rheumatology revised criteria for the classification of systemic lupus erythematosus. *Arthritis Rheum*. 1997;40(9):1725.
59. Zhao M, et al. IL-6/STAT3 pathway induced deficiency of RFX1 contributes to Th17-dependent autoimmune diseases via epigenetic regulation. *Nat Commun*. 2018;9(1):583.
60. Ma CS, et al. Early commitment of naïve human CD4(+) T cells to the T follicular helper (T(FH)) cell lineage is induced by IL-12. *Immunol Cell Biol*. 2009;87(8):590–600.
61. Wu R, et al. MicroRNA-210 overexpression promotes psoriasis-like inflammation by inducing Th1 and Th17 cell differentiation. *J Clin Invest*. 2018;128(6):2551–2568.
62. Xu L, et al. The transcription factor TCF-1 initiates the differentiation of T(FH) cells during acute viral infection. *Nat Immunol*. 2015;16(9):991–999.